

Transients Resulting from the Merger of Degenerate Objects

Chenchong Zhu

`cczhu@astro.utoronto.ca`

May 4, 2011

1. Introduction

The problem of double-degenerate mergers is one that has been well-studied numerically, statistically and observationally. Since there is a well-defined parameter space of possible white dwarf (WD) and brown dwarf (BD) binary systems, it is relatively easy to categorize all possible merger types. In this report, we will survey the observational characteristics and statistics of double-degenerate mergers. We will classify these mergers according to the chemical composition of the more massive of the merging WDs and BDs.

1.1. Population Statistics

WD mass and composition are both dependent on the evolutionary path of the WD progenitor star. A $0.15 - 0.45 M_{\odot}$ WD will have a core comprised mostly of helium, a $0.45 - 1.1 M_{\odot}$ WD will have a core of carbon and oxygen, and a $1.1 - 1.4 M_{\odot}$ WD will have an oxygen-neon-magnesium core (Loren-Aguilar et al. 2009; Marsh 2011). (Work has been done, however, to show that these ranges are not set in stone; eg. Moroni & Straniero (2009).) Brown dwarfs have masses of $\sim 0.08 M_{\odot}$ or lower (Stamatellos & Whitworth 2008).

Close-in WD binaries are the result of common envelope evolution earlier in the binary's history. Gravitational radiation or magnetic braking then drives the binary into a semi-detached state (Motl et al. 2007; Nelemans et al. 2001). It is estimated that there are on order of $10^7 - 10^8$ such semi-detached systems in the Milky Way alone (Motl et al. 2007; Nelemans et al. 2001; Marsh 2011). Therefore any transients created by mass transfer within such systems should be frequently observed.

Statistically, mergers of certain types of WD binaries from Fig. 1 will dominate over others. According to Tremblay & Bergeron (2009), the mass distribution of DA white dwarfs (which comprise the vast majority of WDs) is narrowly peaked around $M = 0.65 M_{\odot}$. This suggests that the majority of WD binary interactions will be between near equal-mass CO WD pairs. Binary evolution, however, will skew the population statistics of binary

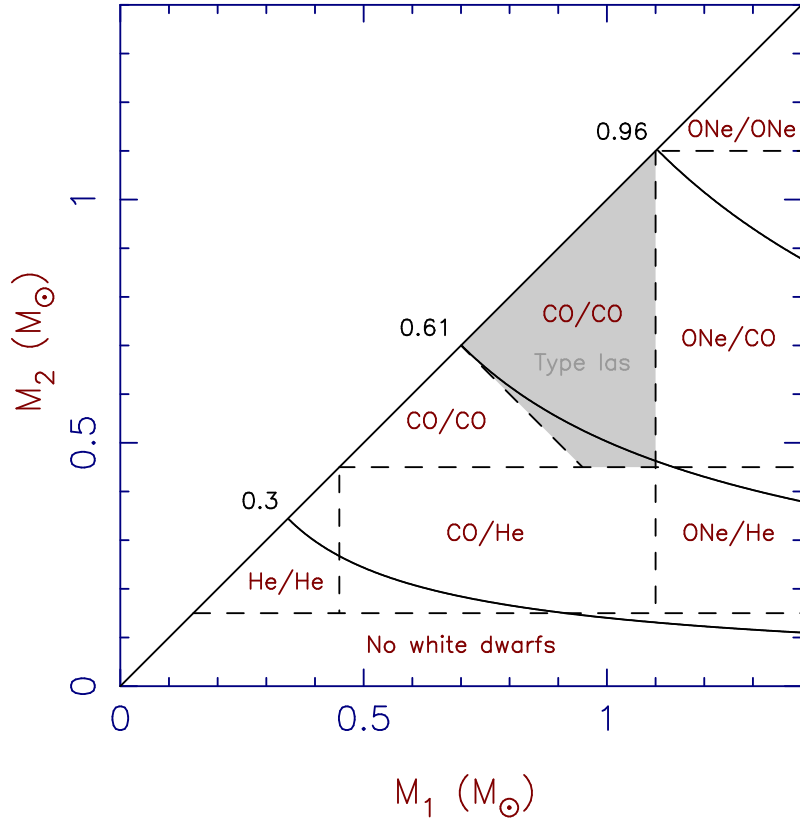


Fig. 1.— Plot of mass ratio ranges for WD binaries of various compositions. Compositions were assumed to map uniquely onto mass via: He = $0.15 - 0.45 M_{\odot}$, CO = $0.45 - 1.1 M_{\odot}$, and ONe = $1.1 - 1.4 M_{\odot}$. These values should be taken as guidelines, and not strict delineations between chemical compositions. The curves are lines of constant gravitational wave chirp mass for inspiralling binaries. The shaded region contains all CO WD binaries whose total mass is equal to or exceeds M_{Ch} , and are therefore expected to cause SNe Ia (see Sec. 5 for details. From Marsh (2011), their Fig. 1.

constituents.¹ Han (1998) uses Monte Carlo simulations of binary evolution to determine that the birth rate of close-in WD binaries in the Milky Way is $\sim 3 \times 10^{-2} \text{ yr}^{-1}$, with 63% being He-CO WD binaries, ~2% He-He, and 35% CO-CO. Han also gives merger rates: $5.7 \times 10^{-3} \text{ yr}^{-1}$ for He-He, $1.81 \times 10^{-2} \text{ yr}^{-1}$ for He-CO and $5.7 \times 10^{-3} \text{ yr}^{-1}$ for CO-CO mergers. Nelemans et al. (2001)'s population synthesis models give different values for birth rates: a total rate of $4.8 \times 10^{-2} \text{ yr}^{-1}$, with 53% of the binaries containing two He WDs, 25% containing two CO WDs (including hybrid CO WDs with thick He envelopes), 20% containing a CO and an He WD, and ~1% containing ONeMg WDs. The total merger rate for WDs of all sorts is $2.2 \times 10^{-2} \text{ yr}^{-1}$. The differences between the two studies can be attributed to different common envelope inspiral efficiencies and treatments of mass transfer and stellar evolution. (Each author also had multiple models with different treatments of such factors as star formation, WD cooling, etc.)

The frequency of BD-BD and BD-WD mergers has not been, to the best of our knowledge, quantified.

1.2. Stability of Mass Transfer

Another factor to consider is the stability of mass transfer between the binary constituents - if mass transfer is stable, then no merger will occur. Stability depends critically on the mass ratio $q = M_2/M_1$ between the donor star (M_2) and the accretor star (M_1), and whether or not spin and orbital angular momentum can be efficiently coupled to each other. We sketch a simple argument for stability in this section. Marsh et al. (2004) has performed more detailed analysis of binary stability, and give more accurate stability criteria in agreement with the argument made here.

We first consider the case in which some process, for example tides or magnetic induction, is able to return spin angular momentum to orbital angular momentum, thus helping to stabilize mass transfer, meaning that (on the timescales of the merger) $\dot{J}_{orb} = 0$. The orbital angular momentum of a binary system is $J_{orb} = (M_1 M_2 / M) \sqrt{GMa}$, where $M = M_1 + M_2$ and a is the orbital separation. From this we may derive $\dot{J}_{orb}/J_{orb} = \dot{M}_1/M_1 + \dot{M}_2/M_2 - \dot{M}/2M + \dot{a}/2a$. We shall assume conservative mass transfer (this is

¹For example, in almost all cases a main-sequence binary system will undergo two stages of mass transfer to create a double degenerate system (one for the giant phase of each star). The first phase of mass transfer must not result in common-envelope evolution; this requires a near-unity mass ratio between the two MS stars (see Van Kerkwijk et al. (2010) for details). The most likely merger, then, is between two WDs of similar mass.

backed by the simulations in Sec. 1.5, which show less than 1% of stellar material becomes unbound even by extremely super-Eddington mass transfer), meaning $\dot{M}_1 = -\dot{M}_2$. Putting this together gives us

$$\dot{J}_{orb}/J_{orb} = 2(q-1)\frac{\dot{M}_2}{M_2} - \frac{\dot{a}}{a}, \quad (1)$$

noting that $\dot{J}_{orb}/J_{orb} = 0$. We use Paczynski's estimate for the Roche lobe of M_2 , $R_L \approx 0.46a(M_2/M)^{1/3}$, valid for $q \lesssim 1$ (Eggleton 1983). Differentiating and using Eqn. 1, we obtain

$$\frac{\dot{R}_L}{R_L} = 2(q - \frac{5}{6})\frac{\dot{M}_2}{M_2}. \quad (2)$$

If we estimate a WD equation of state as a polytrope with $n = 3/2$, we obtain a mass-radius relation (Motl et al. 2007)²

$$R \propto M^{-1/3}. \quad (3)$$

Assuming the constant of proportionality is the same for all WD equations of state, this indicates the less massive white dwarf overflows its Roche lobe first during any mass transfer, validating the use of Eqn. 2 (as all mass transfer will have $q \lesssim 1$) (Camenzind 2009). This results in the WD losing mass and expanding further per Eqn. 3. The counteracting effect is increase in binary orbital separation due to the fact that the lower-mass WD is the donor star (Eqn. 1). We can take the derivative of Eqn. 3 to obtain for the donor star $\dot{R}_2/R_2 = -\dot{M}_2/3M_2$. Comparing this expression to Eqn. 2, and requiring that R_2 expands more slowly than R_L , we obtain the following criterion for stability:

$$2(q - \frac{5}{6}) < -\frac{1}{3} \rightarrow q < \frac{2}{3}. \quad (4)$$

If spin and orbital angular momentum coupling is negligible, a similar analysis can be performed, using total angular momentum $J = J_{orb} + J_{spin} = (M_1M_2/M)\sqrt{GMa} + J_{spin}$, from which we may derive $\dot{J}/J_{orb} = \dot{M}_1/M_1 + \dot{M}_2/M_2 - \dot{M}/2M + \dot{a}/2a + \dot{J}_{spin}/J_{orb}$ (Marsh

²Note this is an equilibrium mass-radius relationship, which may not be a good approximation for a WD undergoing mass transfer. See Loren-Aguilar et al. (2009) for an semi-analytical treatment that takes this into account.

et al. 2004). Following Marsh et al. and Nelemans et al., we assume only the spin of the accretor matters for the equation, and follow Verbunt & Rappaport (1988)’s representation of the spin-up of the accretor from direct impact accretion with $\dot{J}_{spin} = -\sqrt{GM_1R_h}\dot{M}_2$ (\dot{M}_2 is negative). R_h is the effective radius of the matter transferred onto the accretor, and is given by a fitting formula: $R_h = a(0.0883 - 0.04858 \log(q) + 0.11489 \log^2(q) + 0.020475 \log^3(q))$, valid for all plausible WD binary mass ratios (Verbunt & Rappaport 1988). Dividing this by J_{orb} to obtain $\dot{J}_{spin}/J_{orb} = -\sqrt{(1+q)r_h}\dot{M}_2/M_2$, we recognize that mass transfer is conservative ($\dot{J} = 0$), and obtain (Marsh et al. 2004; Nelemans et al. 2001)

$$\frac{\dot{a}}{a} = 2(q - 1 + \sqrt{(1+q)r_h})\frac{\dot{M}_2}{M_2}, \quad (5)$$

where $r_h = R_h/a$. Using the same argument that gave us Eqn. 4, we may obtain a new stability criterion (Nelemans et al. 2001; Verbunt & Rappaport 1988)

$$2(q - \frac{5}{6} + \sqrt{(1+q)r_h}) < -\frac{1}{3} \rightarrow q \lesssim 0.219. \quad (6)$$

Fig 2 from Dan et al. (2011) summarizes this, indicating the zone of guaranteed instability given by Ineq. 4, and the boundary between direct impact accretion and disk accretion (calculated from Nelemans et al. (2001)). Disk accretion results in good coupling between orbital and spin angular momenta, and since the region falls below Ineq. 4, it is definitely stable. (See section 4.5 of Marsh et al., however, for evidence that disk accretion does not stabilize mass transfer at all; the fact that disk accretion systems are stable would then be largely due to Ineq. 6.) This leaves a large region of direct impact accretion in the middle of the two stability regions that may or may not be stable - if no coupling returns spin angular momentum to orbital angular momentum, most of the region should be unstable, as given by Ineq. 6. Marsh et al. (2004) find that the stability in the middle region is dependent primarily on the synchronization timescale of the binary system, a conclusion supported by Gokhale et al. (2007)’s stability analysis³. Unfortunately tidal interaction in WD binaries is not well understood (see Sec. 1.3).

A number of numerical studies have been performed to explore mass ratios of uncertain mass transfer stability, and the results have not been conclusive (Marsh 2011). For example, Motl et al. (2007) used a (grid-based) self-consistent field method to determine that for a

³Another fact that needs to be considered is that even in unstable mass transfer, if the donor can survive long enough for q to drop to a value conducive to stable mass transfer, ultimately the system does not merge (Gokhale et al. 2007)

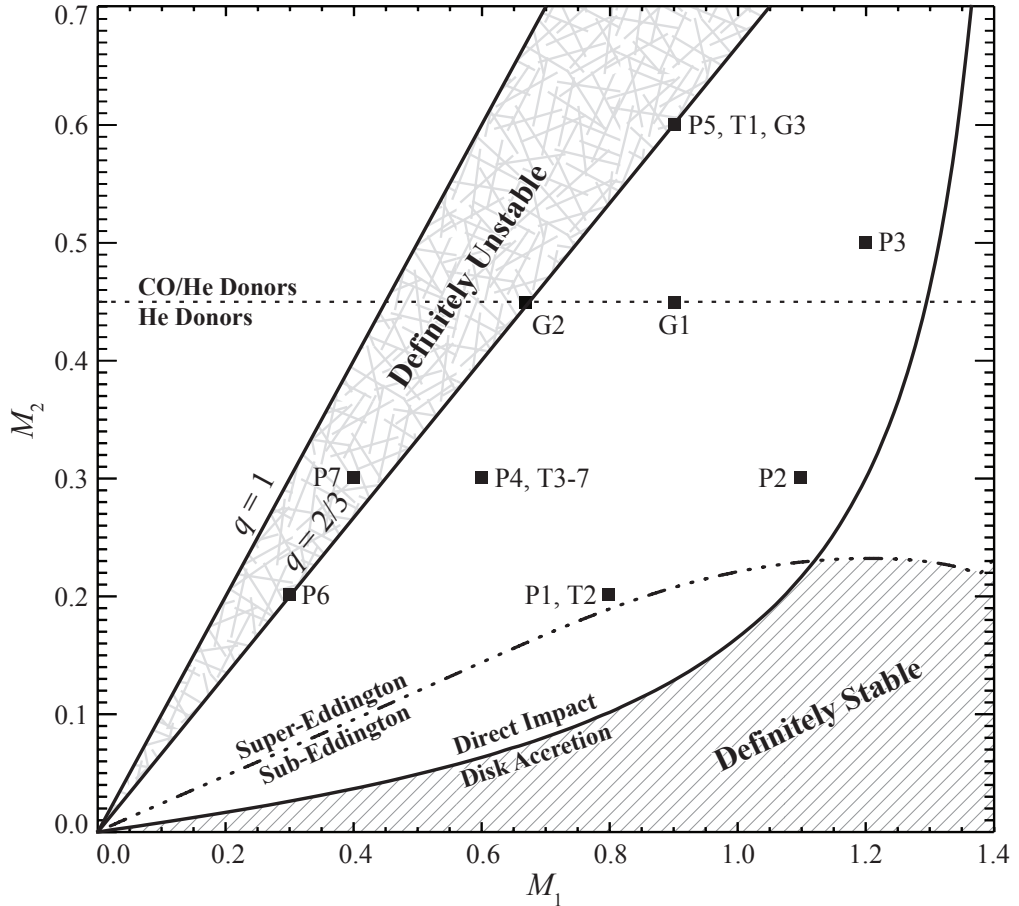


Fig. 2.— Stability of mass transfer parameterized by the masses of the donor and accretor WDs. The “always unstable” region follows from Ineq. 4, and the “disk accretion”/“definitely stable” region is below Ineq. 6 (Ineq. 6 is not plotted, but falls roughly near the sub-Eddington/super-Eddington boundary). The stability criterion for the middle region should fall between Ineqs. 4 and 6. Han & Webbink and Marsh et al. both consider all super-Eddington accretion systems to result in merger, while Gokhale et al. suggest that accretion that is initially super-Eddington may eventually stabilize. SPH simulation conducted by Dan et al. was performed for mass ratios indicated by squares and labels - all these systems merged, though P1 and P2 required several tens of orbits before doing so. From Dan et al. (2011), their Fig. 1.

synchronized system with initial mass ratio $q_{\text{init}} = 0.4$ there is enough spin-orbit momentum coupling to ensure stability. On the other hand SPH simulations of synchronized systems by Dan et al. (2011) using the Helmholtz equation of state yielded a merger for $q = 0.4$, and have shown unstable mass transfer for binaries down to $q = 0.25$. Dan et al. also show that for such mergers a careful construction of the initial conditions results in a long period of mass transfer (several tens of orbital periods) before full disruption of the donor, suggesting that their results can be compatible with the results from (Motl et al. 2007). For the purposes of this paper, we will consider an extreme mass ratio merger to be a plausible (if rare, given WD mass distribution statistics) occurrence.

MARTEN: I'm not sure why the studies I cited all assume synchronized binaries, when no one knows if WDs are synchronized or not, and most people seem to think they aren't.

It should be noted that Dan et al. (2011) also show that merger simulations are sensitive to initial conditions, and point out that the approximate initial conditions of other simulation groups such as Loren-Aguilar et al., Guerrero et al. and Pakmor et al. (2010) may distort their findings. This not only applies to merger stability and merger timescales, but also central temperatures of post-merger remnants.

1.3. Synchronization

Estimates of the synchronization timescale in binary systems give $\tau_S \sim 10^{12}$ yr from radiative damping, and $\tau_S \sim 10^{15}$ yr from viscosity (Marsh et al. 2004). To compare, the timescale for angular momentum loss from gravitational wave radiation is (Segretain et al. 1997)

$$\tau_{\text{grav}} = 5 \times 10^5 \left(\frac{a}{10^5 \text{ km}} \right)^4 \frac{M_\odot}{M_1} \frac{M_\odot}{M_2} \frac{M_\odot}{M_1 + M_2} \text{ yr.} \quad (7)$$

In the latter stages of evolution, this value is around $\tau_S \sim 10^6$ yr. It is then likely that neither donor nor accretor are synchronized at the time of merger⁴. Turbulent viscosity and non-radial mode excitation, on the other hand, can potentially have $\tau_S \ll 500$ yr, and even small magnetic fields, properly oriented, can significantly enhance viscosity (Marsh et al. 2004; Iben et al. 1998). Also, the viscous timescale scales as a^6 , while Eqn. 7 scales as a^4 ; this indicates that should viscosity ever synchronize a WD binary, this binary will be

⁴A close-in WD binary should merge within 10^8 to 10^9 yrs after formation (Segretain et al. 1997). Of course, any transients caused by mergers seen today must have occurred within this time!

synchronized for the remainder of its inspiral (Iben et al. 1998). Whether or not a binary will be synchronized is still largely an unsolved problem (Marsh 2011).

If we were to suppose a WD system could synchronize, then viscous dissipation should heat up both WDs significantly. Iben et al. (1998) perform long equal-mass binary evolution calculations that assumes the binary system is synchronized, and the rate of tidal heating is equal to the rate of spin kinetic energy increase. (SO DOES IT SAP ROTATION????) They find that over the course of the last 10^4 yrs before merger heating from synchronization can increase the temperature of a $1.0 M_{\odot}$ WD (with a $1.0 M_{\odot}$ WD companion) by an order of magnitude. While most of the thermal energy that is radiated away during this heat-up is in the form of neutrinos, the EM luminosity increases by almost five orders of magnitude. At the time of merger, each $1.0 M_{\odot}$ WD would shine with $\sim 100 L_{\odot}$ and have a temperature of $\sim 10^8$ K, making the system a significant X-ray source. The luminosity just before merger increases with WD mass, and the period of time over which luminosity increase occurs drops with WD mass: a $0.3 M_{\odot}$ with an equal-mass companion will increase in luminosity by two orders of magnitude over 10^6 yr. If the efficiency by which rotational energy is converted to thermal energy is reduced to 10% the maximum efficiency in the $1.0-1.0 M_{\odot}$ binary, the final luminosity drops by a factor of about 1000. In all cases simulated, Iben et al. found temperatures were insufficient to ignite nuclear fusion. The periods of increased luminosity are all in the range of $10^2 - 10^6$ years, which, while short compared to the lifetime of the binary, are far too long to be considered transients.

1.4. Super-Eddington Mass Transfer

The luminosity of the accretion flow is set by the amount of energy liberated from transferring M_2 's mass from the inner Lagrange point to the surface of the accreting star. Therefore, $L_{acc} = \dot{M}_2(\phi_{L1} - \phi_{R1})$ (Han & Webbink 1999). For many values of q , however, mass transfer will be higher than the Eddington mass transfer limit. Han & Webbink analytically investigated super-Eddington accretion between compact objects, and concluded that under these conditions, the luminosity is truncated at the Eddington luminosity of $L_{Edd} = 4\pi GM_1 m_p c / \sigma_T$, where σ_T is the Thomson scattering cross-section and m_p is proton mass, while the rest of the energy either goes into mass ejection or is retained as thermal energy. They further find that often less than 50% of the mass of the accretion stream is ejected from the system.

The Eddington mass accretion rate can be estimated by equating L_{acc} with $2L_{Edd}$ (where the factor of 2 takes into account two proton masses for every free electron, as is appropriate for fully-ionized He or CO) to obtain (Marsh et al. 2004)

$$\dot{M}_{Edd} = \frac{8\pi GM_1 m_p c}{\sigma_T (\phi_{L1} - \phi_{R1})}. \quad (8)$$

Steady-state mass transfer rates, assuming perfect coupling between spin and orbit angular momentum, can be determined by equating $\dot{R}_2/R_2 = \dot{R}_L/R_L$, and using Eqns. 1 and 2 to obtain

$$\dot{M}_{acc} = M_2 \frac{\dot{J}_{orb}/J_{orb}}{2/3 - q}. \quad (9)$$

The value of \dot{J} can be assumed to be $\dot{J}_{GR} = -(32/5)(G^3/c^5)(M_1 M_2 M/a^4)J_{orb}$ due to gravitational wave emission (J_{orb} was defined in Sec. 1.2). Equating Eqns. 8 and 9 can be used to estimate the sub-Eddington/super-Eddington mass accretion rate transition in Fig. 2 (see more accurate estimates in eg. Gokhale et al.).

The thermal energy retained by the WD causes the outer envelope to expand, resulting in the creation of a common envelope that leads to runaway mass transfer and a merger (Han & Webbink 1999). This expectation is used in all the stability studies cited in this paper, though it has not been conclusively proven (Motl et al. 2007; Marsh et al. 2004; Gokhale et al. 2007).

The light curve of a merger would consist of a combination of the Eddington luminosity, convolved with effects from radius expansion, and cooling of the ejected mass, which can be estimated via Arnett’s method. This is done in Sec. 1.6.

1.5. Mechanics of WD Mergers

Guerrero et al. (2004), Yoon et al. (2007) and Loren-Aguilar et al. (2009) performed a sampling of high-resolution ($\sim 4 \times 10^5$ particle) SPH simulations of WD mergers. In all three works, the binaries are assumed to be non-synchronized, per Segretain et al.. Earlier simulation work on such mergers were marred by issues of excess artificial viscosity, which more modern studies have attempted to rectify by using more complex prescriptions of viscosity. In particular, Guerrero et al. uses a Balsara switch (which they noted may have been insufficient), Yoon et al. an adaptive viscosity method and Balsara switch, and Loren-Aguilar et al. a method based off of Reimann-solvers plus a switch. Table 1 summarizes their results.

In general the mergers simulated all finish within several orbital periods - this is in

Table 1: Table of WD merger simulation results from Guerrero et al. (2004), Loren-Aguilar et al. (2009), Yoon et al. (2007), Pakmor et al. (2010) and Dan et al. (2011). M_{bin} is the binary system total mass, written as a sum of the binary’s constituent masses, M_{rem} is the mass of the merger remnant, M_{disk} the Keplerian disk, and M_{ej} ejected mass, all of which are in units of M_\odot . The mass-composition relationships given in Sec. 1.1 are used for all runs, unless otherwise indicated. T_{max} is the maximum temperature achieved during the merger, while T_{rem} is the maximum temperature of the remnant. Guerrero et al. only gives final remnant temperatures in a few cases, and final temperatures from two of Dan et al.’s runs were determined from plots. Note that because Guerrero et al. only used a Balsara switch, and did not use equal-mass SPH particles in their runs, which will lead to artificially high viscosities and numerical artifacts Loren-Aguilar et al. (2009). Dan et al. use synchronized systems. Between the three runs, it is consistently shown that nuclear burning is negligible for CO-CO mergers, while Loren-Aguilar et al. found significant non-explosive nuclear processing for He-CO and CO-ONeMg mergers.

Group	M_{bin}	M_{rem}	M_{disk}	M_{ej}	T_{max} (K)	T_{rem} (K)	E_{nuc} (ergs)
Loren-Aguilar et al.	0.3+0.5	0.62	0.18	10^{-3}	6×10^8	6×10^8	1×10^{42}
	0.4+0.8	0.92	0.28	10^{-3}	6.5×10^8	6×10^8	1×10^{44}
	0.6+0.6	1.10	0.10	10^{-3}	6.3×10^8	6.2×10^8	0
	0.6+0.8	1.10	0.30	10^{-3}	1.6×10^9	8.7×10^8	1×10^{41}
	0.6+1.2	1.50	0.30	10^{-3}	1.0×10^{10}	1.0×10^9	2×10^{44}
Yoon et al.	0.6+0.9	1.10	0.40		1.7×10^9	5.6×10^8	1×10^{45}
Guerrero et al.	0.4+0.4			0	2.2×10^8	1.6×10^8	
	0.4+0.6			3.32×10^{-3}	7×10^9		
	0.4+1.2			3.54×10^{-2}	3.1×10^9		
	0.6+0.8			2.82×10^{-3}	1.4×10^9	5×10^8	
	0.6+1.0			6.48×10^{-3}	1.6×10^9		
	0.8+1.0			6.52×10^{-3}	2.0×10^9		
Pakmor et al. (2010)	0.89+0.89			2.9×10^9			
Dan et al.	0.2+0.3			5×10^{-5}	2.37×10^8		
	0.2+0.8			8.6×10^{-3}	4.89×10^8	4.5×10^8	
	0.3+0.4			6.5×10^{-4}	2.72×10^8		
	0.3+0.6			3.7×10^{-3}	4.92×10^8		
	0.3+1.1			1.76×10^{-2}	1.223×10^9		
	0.45+0.67			9×10^{-4}	1.23×10^9		
	0.45+0.9			4.6×10^{-3}	1.611×10^9		
	0.5He+1.2			1.74×10^{-2}	1.885×10^9		
	0.6+0.9			1.85×10^{-3}	1.06×10^9	5.6×10^8	
	0.9+1.2CO			3.4×10^{-2}	7.115×10^9		

contrast to the simulations done by Motl et al. and Dan et al., and is likely due to a choice of initial conditions. When the two WDs begin the merger process, the less massive WD fills its Roche lobe and begins to transfer mass (as expected), is completely disrupted tidally, and eventually forms an outer envelope and a fat disk around the more massive WD (due to highly super-Eddington accretion, most of the material is not incorporated into the larger WD). During this time temperatures often reach 10^{11} K at the point of contact between the accretion stream and the more massive WD, initiating nuclear reactions, but they are quickly quenched as this region expands, loses degeneracy, and cools. Loren-Aguilar et al. notes the expanding material then redistributes itself over the surface of the more massive WD, forming a “hot corona”. Loren-Aguilar et al. and Yoon et al. both find rigidly rotating cores, differentially rotating outer remnant layers (spun up by the merger) and sub-Keplerian disk, while Guerrero et al. finds a completely rigidly rotating remnant (likely due to just using a Balsara switch). Loren-Aguilar et al. also perform a $0.6\text{-}0.6 M_{\odot}$ CO WD equal mass merger, and Guerrero et al. perform a $0.4\text{-}0.4 M_{\odot}$ He WD merger, with both observing noticeable differences from unequal mass mergers. No real “disk” is formed, though the merger remnant has an extended ellipsoidal shape, and the peak temperature is near the centre of the remnant instead in the hot corona. Additionally, the entire remnant rigidly rotates. In all simulations presented, very little ($< 10^{-3} M_{\odot}$) mass is ejected from the system.

Nuclear burning in the merger simulations produces energies ranging from 10^{42} to 10^{45} ergs, and Loren-Aguilar et al. note 10^{21} to 10^{37} ergs are emitted as neutrinos (a strong function of merger mass), and 10^{39} to 10^{41} ergs are emitted as gravitational waves. As the amount of ejected mass is minimal, photon emission should roughly be Eddington luminosity limited, and therefore is also orders of magnitude below the nuclear burning. Nuclear processing is significant for He-CO and CO-ONeMg mergers, while CO-CO mergers have little nuclear processing (Loren-Aguilar et al. 2009).

Pakmor et al. (2010) perform an 0.89-0.89 merger simulation, which qualitatively agrees with the equal mass mergers of Loren-Aguilar et al. and Guerrero et al., and track the hottest points in the system during merger. They find that a detonation should arise from a hotspot with density $3.8 \times 10^6 \text{ g/cm}^3$ and temperature $2.9 \times 10^9 \text{ K}$, resulting in the complete disruption of the system. See Sec. 5 for details.

Dan et al. (2011) also perform merger simulations, though unlike the other simulations they relax to equilibrium their binary system, rather than just each star, to obtain realistic initial conditions, and assume synchronization has occurred. Their results show that approximate initial conditions (also of synchronously rotation systems) tend to overestimate remnant maximum temperatures and densities (as well as underestimate merger times, as mentioned earlier). A few resolution tests were performed with non-rotating systems; these

showed faster merger times and slightly higher remnant maximum temperatures (Dan personal communication 2011). Peak temperature during the merger and ejected mass are reproduced here. It should be noted that maximum temperature values were not found via averaging (Dan personal communication 2011). This runs the risk of overestimating the temperature significantly, as all fluid properties in SPH should be determined by averaging using the kernel.

MARTEN: Do you know if Loren-Aguilar has the same problem finding hotspots? Pakmor doesn't, since they run resolution tests.

Loren-Aguilar et al. also find some particles ejected into highly eccentric orbits, and expect them to emit high-energy photons when colliding with and becoming absorbed into the sub-Keplerian disk. They obtain a light curve for this phenomenon by following a similar calculation for neutron star and black hole merger remnants by Rosswog (2007). The calculation assumes that highly eccentric particles impacting the disk lose all their kinetic energy, and that all this energy is turned into high-energy photons - the light curves should therefore be taken as (extreme) upper limits to the shape of the curve. The transient has a peak luminosity upper limit of $\sim 10^{51}$ erg, but only lasts for several hundred seconds to several tens of hours. Nevertheless, Loren-Aguilar et al. find large luminosities for a wide range of merger mass ratios, and state this would be a tell-tale signature of a WD binary merger. See Fig. 4 for light curves.

1.6. A Merger Light Curve Estimation

Using Arnett's light curve prescription, we can estimate the light curve formed by a merger. Luminosity will come from two sources: the cooling of ejected material and the Eddington-luminosity remnant. We therefore assume either $\sim 10^{-3} M_{\odot}$ or $\sim 2 \times 10^{-2} M_{\odot}$ of non-radioactive ejecta with input energy from an Eddington-luminosity remnant, the mass of which is varied. Ejecta velocity is assumed to be the escape velocity. Ejecta composition (important for recombination) is in accordance with those stated for Fig. 1. For He, we use a recombination energy of 24.6 eV and a recombination temperature of 10^4 K. For CO, we follow Arnett's estimate of simply using 13.6 eV and 7500 K.

The result is a very weak transient whose luminosity is often just the assumed Eddington luminosity of the central remnant (obviously, this luminosity will decrease over time as accretion ceases; this decline is not modelled), with a maximum peak caused solely by liberated photons during recombination. Fast recombination is assumed in this experiment - slow recombination might give different peak values and rise times.

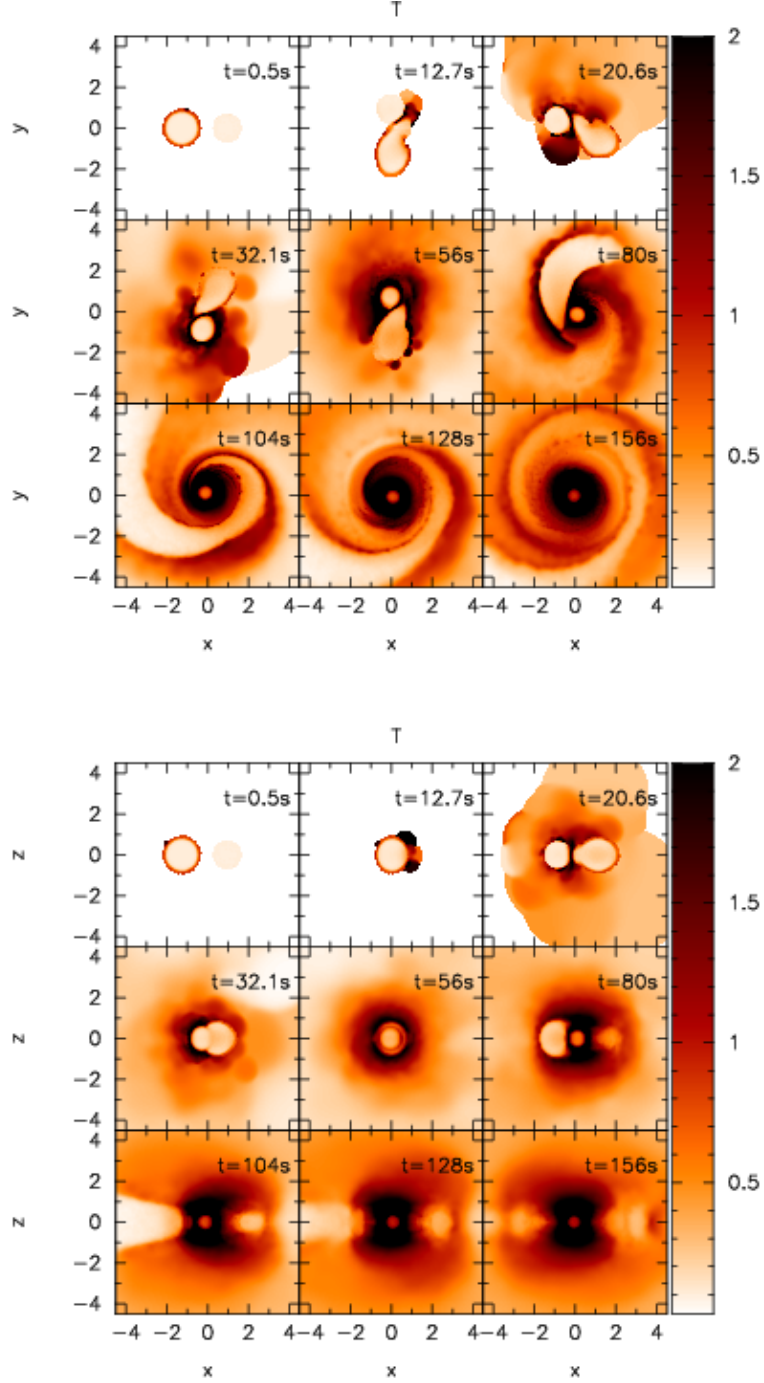


Fig. 3.— xy and xz plane plots of the merger between a 0.6 and a $0.8 M_{\odot}$ CO WD at different times. Colours indicate different temperatures. The creation of a hot corona is quite evident in the xz plane plot. From Loren-Aguilar et al. (2009), their Fig. 2.

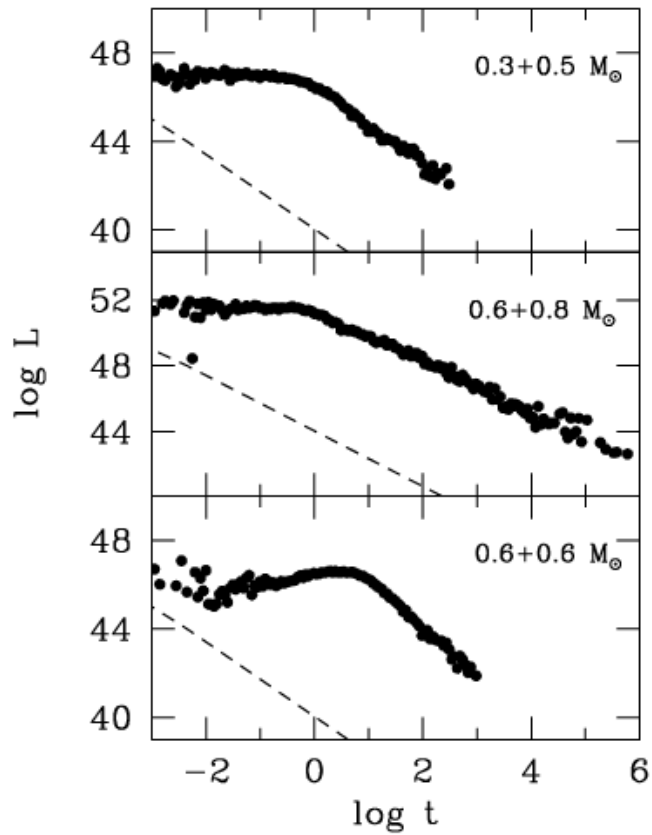


Fig. 4.— Plot of bolometric luminosity versus time for high-eccentricity material falling onto the Keplerian disk. These plots set upper limits to the luminosity over time (real values may be orders of magnitude lower). From Loren-Aguilar et al. (2009), their Fig. 8.

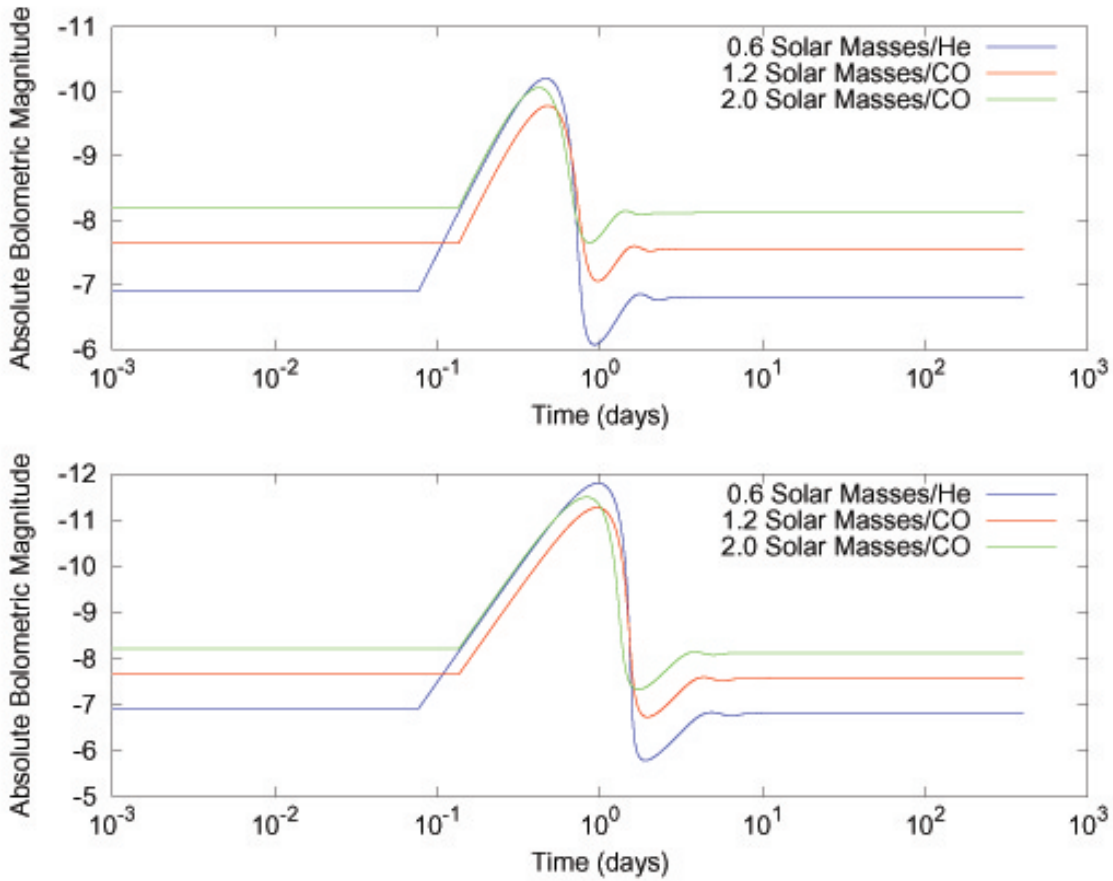


Fig. 5.— Bolometric light curves vs. time calculated using an implementation of Arnett’s semi-empirical explosion model. Absolute magnitudes were calculated with Vega as $M = 0$. The top figure assumes $10^{-3} M_{\odot}$ of He or CO ejecta travelling at escape velocity from a $0.6 M_{\odot}$ He, $1.2 M_{\odot}$ CO or $2.0 M_{\odot}$ CO remnant (remnant and ejecta have the same composition). The bottom figure assumes $10^{-2} M_{\odot}$ of ejecta. Peak light for $10^{-3} M_{\odot}$ is ~ -10 mag at ~ 0.5 days. Peak light for $10^{-2} M_{\odot}$ is ~ -11.5 mag after ~ 1 day.

It has been found, then, that in general mergers themselves do not (except in the cases of Pakmor et al. (2010) and the eccentric material fallback transient Loren-Aguilar et al. (2009)) produce appreciable transients. It is still an open question whether, post-merger, the accretion of the hot disk onto the remnant core will result in a transient. We now explore this possibility.

2. Brown Dwarf Mergers

2.1. With Brown Dwarfs

The existence of BD-BD binary systems has been observationally well-established. Since neither object has ever underwent steady H-fusion, common-envelope evolution cannot be used to create a close-in BD-BD system - this requires other mechanisms, such as three-body interactions, to come into play (D'Angelo et al. 2006; Bear et al. 2011). As exactly how BD and BD systems are formed is still being debated, such a scenario cannot be ruled out (Bear et al. 2011).

Bear et al. (2011) has studied the merger of a BD with a $1 - 10 M_J$ gas giant. Despite the mass ratio q being tiny, the density difference between the two objects means that a gas giant can actually approach a BD until it is tidally disrupted and forms an accretion disk, which falls onto the BD in a matter of several days. This highly super-Eddington accretion powers the light curve. This process is called a “mergeburst”, and similar mergers between main-sequence stars are covered in another section of the report. As this process is qualitatively similar to what was described in Sec. 1.5, it might be useful in describing cold (no nuclear processing) mergers between massive and extremely light BDs. Bear et al. suggests that the light curve of this mergeburst in the V-band will to first order look like a scaled-down version of other intermediate-luminosity optical transients (ILOTs), and scales the V-band light curve of V838 Mon’s ILOT to the parameters of the BD to obtain Bear et al. Eqn. 7. Using this same equation for a $60 M_J - 30 M_J$ BD-BD merger, we obtain a peak V-band luminosity of $10^{38} - 10^{39}$ erg s $^{-1}$ ($\sim 7 - 10$ mag), and a transient timescale (from the disk’s viscous timescale) of a few days.

There are several limitations with this simple scale-up from Bear et al. to a BD-BD merger. For one, more equal-mass BD-BD mergers should disrupt both stars, creating a remnant hottest at its centre - subsequent disk accretion may result in enough compressional heating to ignite central burning, or the stars might even ignite during the merger. An H-flash during accretion followed by steadier nuclear burning might also be possible in cases of unequal mass mergers (see Sec. 3.1 for similar evolution with He). Lastly, any explosive event or violent accretion event should eject material, which will modify light curves. An in-depth study of BD-BD mergers would be needed to address these issues.

MARTEN: My understanding is that mergebursts obtain their energy from shock-heating of material as it plows into the outer atmosphere of the accretor. Since this also happens in WD mergers, should we expect mergerburst like emission, at least at the beginning?

2.2. With White Dwarfs

A number of BD-WD systems are known to exist in nature. Observationally there is, however, a distinct lack of close-in MS-BD systems, a trend known as the “brown dwarf desert” (Stamatellos & Whitworth 2008). The most massive BDs should be $\sim 0.08 M_{\odot}$, while the least massive known WDs are approximately double this value, suggesting that $q = 0.5$ BD-WD systems (unstable by the analysis in Sec. 1.2) may exist (Brown et al. 2011). Note there is extensive work on WDs stably accreting hydrogen-rich material, which is covered in other sections of this report.

Like with BD-BD mergers, our literature search did not find any studies of WD-BD mergers.

3. Helium-Helium White Dwarf Mergers

3.1. SdB Star Formation Channel

Saio & Jeffery (2000) simulated He accretion at $10^{-5} \text{ M}_\odot \text{ yr}^{-1}$ onto 0.3 and 0.4 M_\odot He WDs, which they stated was a rough approximation of the He-He merging process. From Sec. 1.5 it is obvious this is not the case for the initial merger, but such a situation could approximate the accretion of the disk onto the remnant core. Accretion was halted when the WD reached a predetermined mass (between 0.5 M_\odot and twice the initial mass). After a certain mass had been accreted, a He flash results, with a nuclear luminosity on order of 10^{39} to $10^{41} \text{ erg s}^{-1}$. This energy trickles into the envelope and increases the radius and luminosity of the star, which eventually forms a yellow giant after $\sim 10^3$ years. Mass transfer stops during the yellow giant phase, and as the He shell burning continues to propagate inward, the merger remnant evolves (over 10^6 yr) toward the helium main sequence, with additional periodic He shell flashes. The models considered by Saio & Jeffery pass, on a log g vs. log T_{eff} , near the observed position of low-luminosity extreme helium star (EHe) V652 Her, and the models can also reproduce the pulsation and period change, as well as the surface composition, of V652 Her. The star eventually becomes a hot subdwarf B (sdB) star (Saio & Jeffery 2000). Han et al. (2002) obtains similar results, and Han et al. (2003) give the formation rate of sdB stars from mergers, cited below. Follow-up work published in Saio & Jeffery (2002) indicate that He WD mergers combined with heavier CO WDs might account for a much larger fraction of EHes.

It is worth noting that a post-merger remnant He WD would have very different temperatures and mass distributions compared to a cold WD evolved from a single star. It would therefore be worthwhile to repeat such a study using initial conditions explicitly determined from merger simulations.

3.2. Possible Explosive Nuclear Burning?

3.2.1. Statistical Arguments

An accretion rate of $10^{-5} \text{ M}_\odot \text{ yr}^{-1}$ is approximately half the Eddington limit (Saio & Jeffery 2000). Loren-Aguilar et al. (2009) and Van Kerkwijk et al. (2010) both note that the accretion rate could be enormous, which may suggest other evolutionary channels such as a violent core or off-centre He detonation through compressional heating (*a la* Van Kerkwijk et al.’s work on CO WD mergers; see Sec. 5.2.2).

If this were the case, then we would expect that the (calculated) rate of He-He WD mergers that ignite He, which we shall refer to as the “formation rate from mergers”, is much higher than the birth rate of single sdB stars. From Monte Carlo studies of binary evolution, Han et al. gives the rate of sdB formation at $\sim 0.014 - 0.063 \text{ yr}^{-1}$, and the formation rate from mergers at $0.003 - 0.017 \text{ yr}^{-1}$. Observationally the birth rate of sdBs is $\sim 0.01 \text{ yr}^{-1}$, and simulations show the binary fraction for sdBs is around 75% - 90%, giving a value of single sdB star formation roughly consistent with the formation rate from mergers (Nelemans et al. 2001; Han et al. 2003; Heber 2009).

There are, however, multiple methods, both through binary (with main-sequence and sub-stellar companions rather than WDs) and single star evolution, of potentially producing an sdB star (Heber 2009; Nelemans 2010). Nelemans (2010)’s population synthesis study shows that more than 90% of all He WD mergers should be massive enough to ignite He, meaning that many more sdBs are created than single He WDs from mergers. Common-envelope evolution with a sub-stellar companion, on the other hand, produces several times more single He WDs than sdBs. The rate of single He WD formation can be estimated from observations to be $7.5 \times 10^{-14} \text{ pc}^{-3} \text{ yr}^{-1}$ ($\times \sim 5 \times 10^{11}$ for birth rate in the Milky Way), while the birth rate of single sdBs is less than $2 \times 10^{-14} \text{ pc}^{-3} \text{ yr}^{-1}$. This suggests that common-envelope evolution with sub-stellar companions creates the bulk of single He WDs. Nelemans (2010) find that if they assume all single He WDs are formed by common-envelope evolution with sub-stellar companions, enough sdBs are also created to roughly match observed sdB birth rates. This argument appears to leave room for some He-He WD mergers to explode instead of forming sdBs. Further problems, however, arise from the fact that there are also multiple paths to forming not only sdBs but also single He WDs. Details in binary evolution model parameters such as common envelope ejection efficiency vary between papers, which must be accounted for.

It is obvious that due to multiple formation channels it is extremely difficult to tell if there is a discrepancy between the rate of He-He mergers and the rate of sdB star formation from such mergers. Better constrained statistics on merger and formation rates may make such a thought experiment viable in the future.

3.2.2. Light Curve Estimation

Arnett’s light curve formulation can be used to estimate the transient resulting from the detonation of a $0.6 M_{\odot}$ He-He merger remnant. 50% of the star is assumed to fuse via the $3-\alpha$ process, and 50% of the energy released is assumed to go into SN thermal energy (the other 50% goes into kinetic), assuming negligible neutrino losses. A 24.6 eV recombination

energy and a recombination temperature of 10^4 K is used. Analogous to He shell detonations described in Sec. 4.2, the ^{44}Cr decay chain powers the light curve, and is assumed to comprise 10% of the ejecta.

The result is a light curve comparable to weak SNe Ia. Changes to initial energy and ^{44}Cr fraction can shift the final light curve peak light by ~ 2 magnitudes, and change time of peak light by several days. This would suggest that He-He merger remnant explosions, if they occur, could easily be detected. Since ejecta would be composed of a mix of unburned helium and intermediate-mass elements, they would spectroscopically appear very different than canonical SNe Ia.

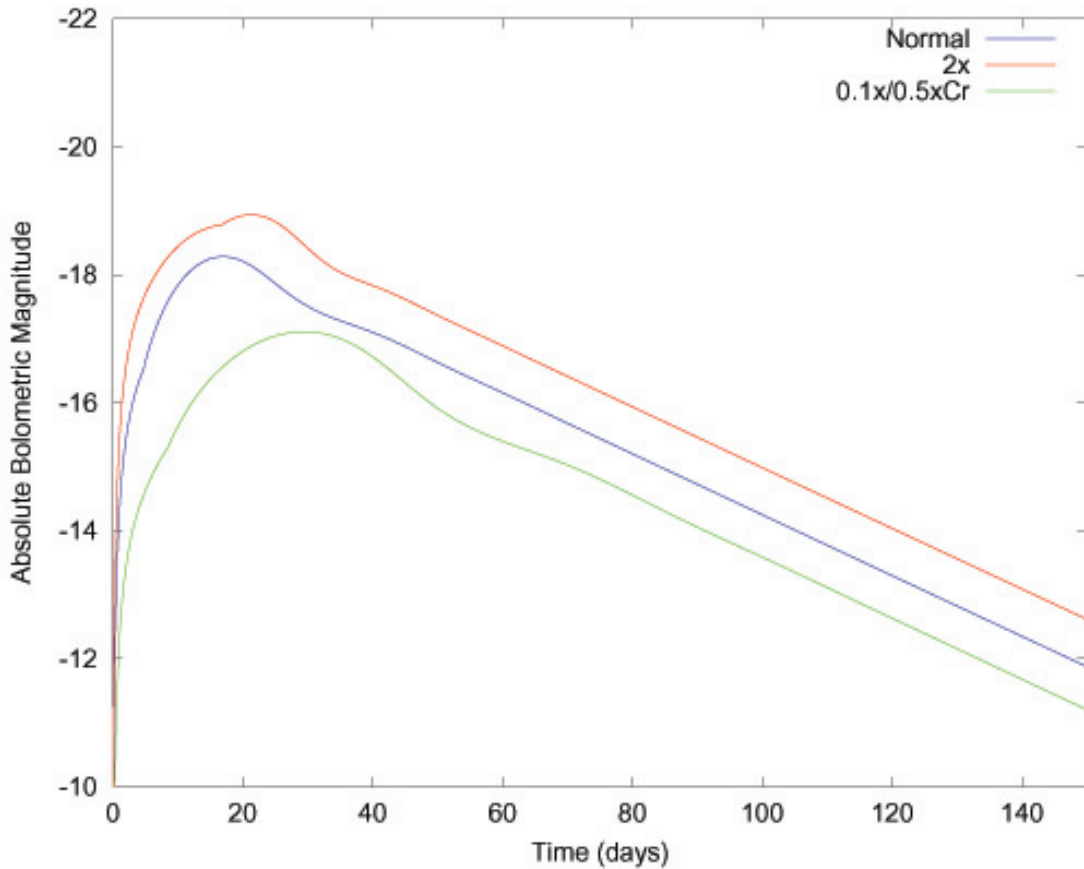


Fig. 6.— Arnett light curve estimate of the detonation of a $0.6 M_{\odot}$ He-He merger remnant. The default explosion assumes $0.6 M_{\odot}$ of ejecta, 10% of which is radioactive ^{44}Cr . Energy is estimated to be 50% of the energy obtained from fusing 50% of the star via the $3-\alpha$ process. Recombination energies and temperatures are set to those of He. Two other light curves are also calculated: one with twice the amount of energy and ^{44}Cr produced as well as the assumption that most of the ejecta is CO (which only changes recombination), and another with ten times less energy and half as much ^{44}Cr . The range of peak light magnitudes obtained is ~ -17 - -19 , and peak light occurs from 15 - 30 days. To compare, canonical SN Ia values are -19.5 mag at ~ 20 days.

4. Carbon-Oxygen WD Mergers With Helium Companions

4.1. Quiet Formation Channels

Following a merger between a CO WD and an He WD, a heavy CO remnant is formed with a hot He envelope and a fat He disk. If the disk accretes at near-Eddington or super-Eddington rates, hydrostatic nuclear burning generally results, as the accretion stream will be hot and will not be very dense. This can be seen from the following argument: from Loren-Aguilar et al. (2009) we obtain a disk temperature of approximately 10^7 K for a $0.3 - 0.5 M_{\odot}$ He-CO merger, and let us assume an accretion rate of $100 M_{\odot} \text{ yr}^{-1}$. Using Figs. 1 and 2 from Bildsten et al. (2007) (reproduced here as Fig. 7), we determine that the amount of mass accreted before He ignition will be less than $10^{-3} M_{\odot}$, meaning that $t_{\text{nuclear}} \ll t_{\text{dynamical}}$, and therefore hydrodynamic burning is never achieved, and the He layer simply expands to accomodate the additional energy generated.

We therefore expect a number of channels for the remnant of a CO-He merger to continue stellar evolution, rather than explode. These channels are discussed below.

4.1.1. Extreme Helium, R Coronae Borealis and Hydrogen-Deficient Carbon Star Formation

Clayton et al. (2007) semi-analytically calculate disk accretion following a merger between a CO WD of variable mass and an He WD of either 0.2 or $0.4 M_{\odot}$. They state that accretion occurs at an average rate of $\sim 30 - 140 M_{\odot} \text{ yr}^{-1}$ (assumed to be steady over time), building up an He atmosphere. The temperature of the atmosphere, $1 - 4 \times 10^8$ K, is high enough to ignite He, and significant nuclear processing results (without explosion, in line with Sec. 1.5) (Clayton et al. 2007). Clayton et al. suggest that “hot” (with nuclear burning) mergers between He WDs and CO WDs will form hydrogen-deficient (HdC) and R Coronae Borealis stars. This is qualitatively suggested by the extremely low isotopic ratio of $^{16}\text{O}/^{18}\text{O} \lesssim 1$ (less than 0.2% solar), indicating significant production of ^{18}O . Clayton et al. perform a nucleosynthesis experiment simulating He burning on the merger remnant atmosphere, and recover similar isotopic ratios as are observationally found in RCrB stars.

Saio & Jeffery (2002) also model the post-merger evolution of a remnant formed by a $0.5 - 0.6 M_{\odot}$ CO and a $0.1 - 0.4 M_{\odot}$ He WD, assuming a mass accretion rate of $10^{-5} M_{\odot} \text{ yr}^{-1}$. Like the He-He merger remnants in Saio & Jeffery (2000), once He burning begins the system evolves toward a yellow giant, during which a series of weak He flashes will occur. Depending on how much He exists above the shell, the star will remain as a yellow

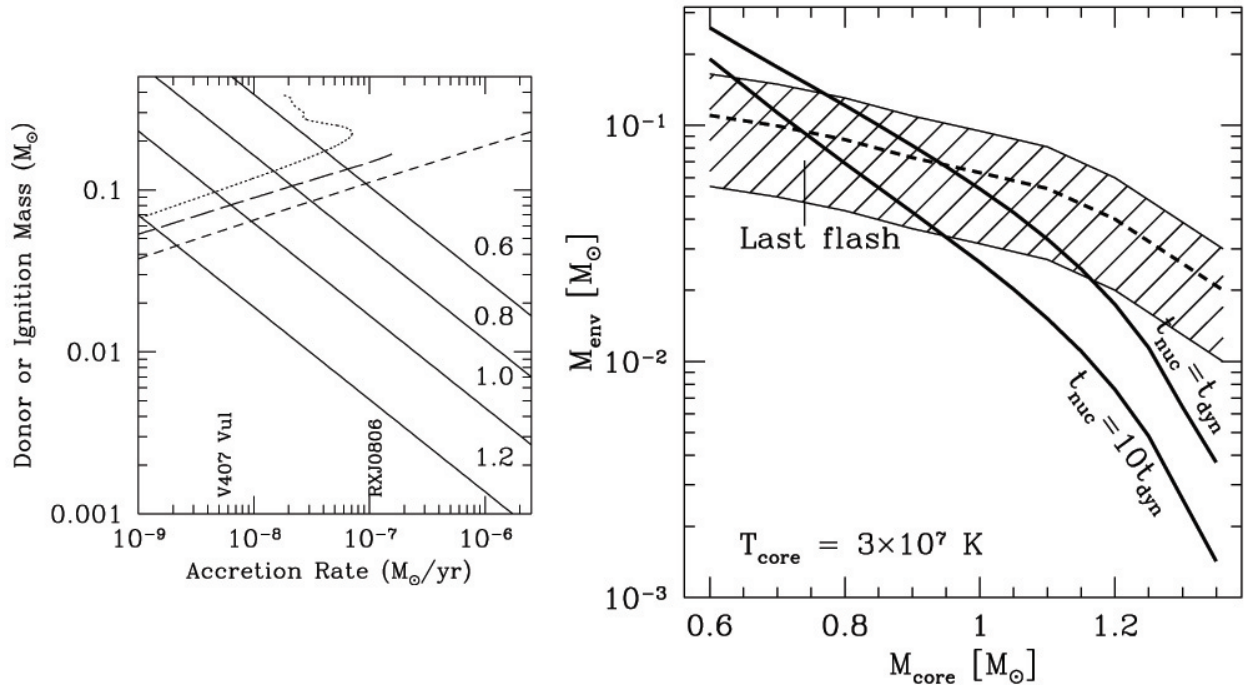


Fig. 7.— Left, estimates (solid lines) for the He ignition mass given accretion of pure He onto a CO WD of 0.6, 0.8, 1 and 1.2 M_\odot . The dashed lines represent fully degenerate (short-dashed) and semi-degenerate (long-dashed) He donor mass given a particular accretion rate, and the dotted line represents the same for a He-burning star. The accretion rate of two particular AM CVn systems is given on the accretion rate axis. Right, the curves $t_{\text{nuc}} = t_{\text{dyn}}$ and $t_{\text{nuc}} = 10t_{\text{dyn}}$ on a plot of envelope vs. core mass , as well as the approximate regime for the last He flash envelope/core mass relationship for AM CVn stars (dashed line is best estimate, hatched region indicate error). Anything to the upper right of $t_{\text{nuc}} = t_{\text{dyn}}$ will result in an explosion. From Bildsten et al. (2007), their Figs. 1 and 2.

giant for some time, before He exhaustion moves the star toward the blue side of the HR diagram. The blueward evolutionary track of the giant on a $\log g$ vs. $\log T_{\text{eff}}$ passes by the values of a number of observed EHe stars. Additionally, luminosities, masses, secular evolution and (broadly) surface compositions of observed EHe stars can be explained by this formation channel. The rate of CO-He mergers (as given by Nelemans et al. (2001)) and the time period over which a remnant will appear to be an EHe combined give a rate of EHe stars in the Milky Way that roughly matches the observed number. This suggests that CO-He mergers are the primary progenitor to EHe stars, and a sizable number of CO-He mergers are quiet.

More recently, Pandey & Lambert (2011) concluded that nucleosynthesis is unnecessary to explain observed abundances of a large number of elements, including ^{18}O . A more detailed analysis by Jeffery et al. (2011) yielded results that do not give either cold or hot mergers a clear advantage in predicting RCrB and EHe star surface abundances. It should be noted, however, that simply from merger simulations some nuclear burning is to be expected - these recent results simply show nucleosynthesis may not matter for EHe/RCrB surface composition.

4.1.2. *SdO Star Formation*

Subdwarf B stars will eventually evolve into post-sdB stars, “hybrid” CO WDs with thick He envelopes. Since one significant binary channel for sdB star formation is a common envelope phase between a giant and a WD, there should be a significant number of sdB stars with close-in He WD companions. Justham et al. (2011) propose that the merger between the He WD and post-sdB star forms a helium-rich subdwarf O star. They take their merger to be the standard core and accretion disk, and then perform a slow accretion of the disk onto the core at a sub-Eddington rate with nuclear burning artificially suppressed. Once the merger is complete, they ignite He fusion, and find that on a $\log g$ vs. $\log T_{\text{eff}}$ plot the majority of the merger product’s life is spent close to the values of observed sdO stars. An order of magnitude estimate from the formation channel statistics of Han et al. (2003) gives similar observed sdO/sdB ratios as is seen in surveys. Since nuclear burning was not treated in full, it is not obvious if He flashes could occur over the course of the remnant’s evolution.

4.2. Helium Envelope Disruption

As shown above, if accretion rates for the disk onto the merger remnant are above $\sim 10^{-5}$, hydrostatic burning ensues. If, however, accretion rates are below $\sim 10^{-6} M_{\odot} \text{ yr}^{-1}$,

a He thermonuclear explosion could result that disrupts the outer He layer of the star - this can also be seen from Fig. 7. If this event is a detonation, known as a Ia supernova, the detonation wave may even travel into the CO core, producing a second, carbon-oxygen, detonation. Accretion rates are critically dependent on the viscosity of the thick post-merger disk. Based on estimates from Loren-Aguilar et al. of the viscous timescale, core accretion could as low as $10^{-10} - 10^{-14} M_{\odot} \text{ yr}^{-1}$ if the viscosity is laminar, or as high as $10^2 M_{\odot} \text{ yr}^{-1}$ if viscosity is turbulent. If we entertain the possibility of very low viscosity rates, then a He envelope disruption becomes much more likely.

Guillochon et al. (2010) suggests another possible explosion channel. During the merger itself accretion rates ranging from $10^{-5} - 10^{-2} M_{\odot} \text{ yr}^{-1}$ will result in shearing within the accreted He envelope, which then creates large-scale Kelvin-Helmholtz instabilities. These instabilities form over-dense regions that periodically compress the inner regions of the envelope, possibly resulting in conditions for detonation. Using the results of SPH simulations, Guillochon et al. (2010) simulate unstable WD binary mass transfer in an adaptive mesh code, and find detonation may be possible on a ($0.6 - 0.9 M_{\odot}$) CO WD that has accreted *sim* $0.1 M_{\odot}$ of He. Guillochon et al. did not study if this process could also occur during post-merger disk accretion.

4.2.1. He Novae and Deflagrations

Woosley & Kasen (2010) carry out an extensive investigation into He shell detonations, including the conditions within the He shell necessary for detonation. An explosion will occur so long as the dynamical timescale is longer than the nuclear timescale. Whether this explosion is a helium nova, or a deflagration or detonation of the entire shell, depends on the convective timescale compared to the "runaway timescale". Woosley & Kasen define the runaway timescale as the time it takes for He (with its current temperature) to rise to extremely high temperatures if convection were artificially turned off. From their simulation results, they take $\tau_{\text{run}} \approx 2 \text{ s}$ to be a good trace of the boundary between nova and detonation/deflagration, which they translate to a relationship between density and pressure. Similarly, to form a detonation shockwave via the Zel'Dovich mechanism requires that the ratio of distance between two points over the difference in their nuclear runaway timescales be larger than the sound speed to create a detonation wave. This translates to (using the assumption of adiabaticity of the temperature gradient) a relationship between density and temperature, which is plotted alongside simulation results in Fig. 8. Simulations show that these semi-analytical estimates should be trusted only to first order.

Below a critical density/temperature given in Fig. 8, convection can effectively carry

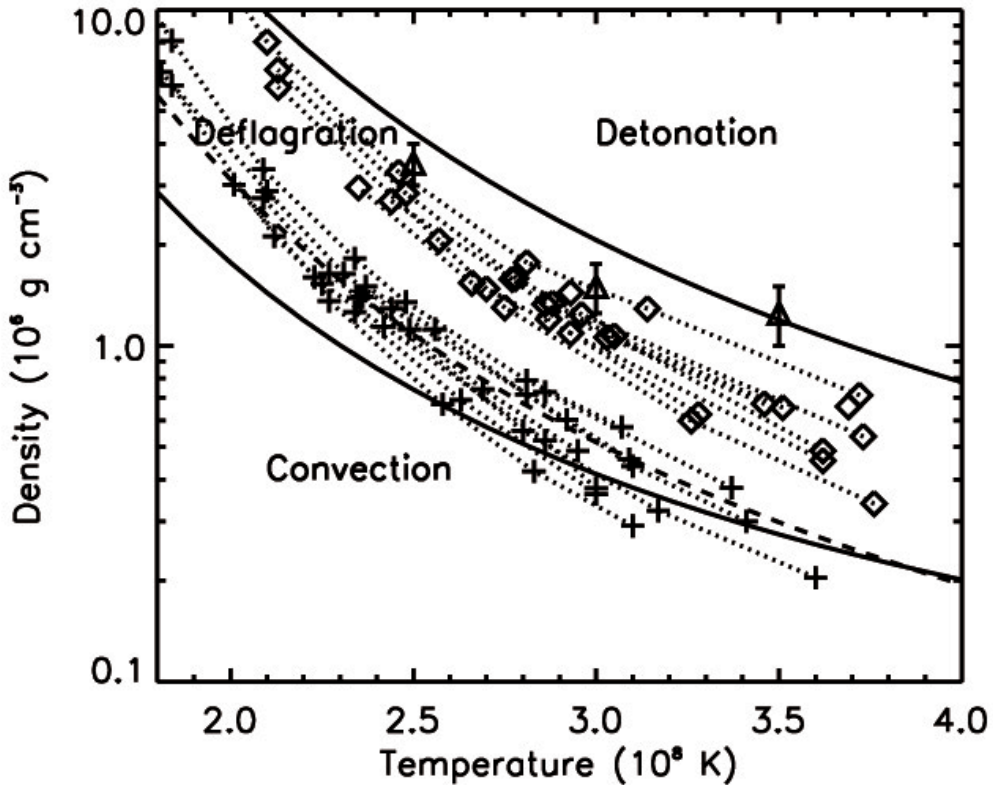


Fig. 8.— A plot of density versus temperature for the He burning region, with the regions for He novae, deflagrations and detonations indicated. Along with the two analytic estimates of the boundaries of the different regions, a number of simulations are also plotted here. Diamonds indicate planar (1D) simulations that eventually reach a thin burning shell luminosity of 10^{47} erg s $^{-1}$, and crosses indicate simulations that achieve 10^{46} erg s $^{-1}$. Dotted lines connecting diamonds/crosses indicate families of simulations for which the accreting CO WD was identical, but the accretion rate is varied. All simulations that reached 10^{47} erg s $^{-1}$ detonated, and most that reached 10^{46} erg s $^{-1}$ deflagrated. Discrepancy between the analytic estimates and the simulations are due to simulations accounting for gas dynamics and utilizing a more correct equation of state. Apparently, dividing the analytic deflagration-detonation border by four (arbitrary value) gives a better fit to the simulations (dotted line). The deflagration-detonation border determined by fine-zone simulations looking single-point detonations are given by triangle points. From Woosley & Kasen (2010), their Fig 2.

away energy from the thin shell, resulting in He novae, which are covered in another section of the report. In the intermediate region between the $\tau_{\text{run}} \approx 2$ condition for explosion and the condition for detonation is the regime for He deflagrations, which are weak (peak B-band magnitude of ~ -15 , ejecta velocities of $\sim 6000 \text{ km s}^{-1}$ for unburned He, and slower for heavier elements), fast-evolving explosions that produce $\sim 0.1 M_{\odot}$ of mostly intermediate-mass elements, or IMEs, ($< 10^{-4} M_{\odot}$ ^{56}Ni) and are powered primarily by ^{48}Cr (Woosley & Kasen 2010). For the two deflagrations simulated by Woosley & Kasen, both ejected most of the accreted He envelope, but processed very little of it. He deflagrations are covered in another section of the report as well.

Note that some of Waldman et al. (2010)’s simulations skirt perilously close to the deflagration regime, while Shen et al. (2010)’s simulations have initial conditions more firmly in the detonation regime.

4.2.2. *He Detonation Without CO Detonation (.Ia Supernova)*

Woosley & Kasen (2010), Shen et al. (2010) and Waldman et al. (2010) all simulate in 1D detonations at the base of the merger remnant He envelope, with CO burning artificially suppressed, and all find the detonation unbinds the entire He outer layer of the remnant, while the CO layer is left relatively intact. Of these, Waldman et al. is particularly interesting due to the higher mass ratio between the CO core and He shell (which would more likely for a merger). Waldman et al. explore a range of CO core ($0.45 - 0.6 M_{\odot}$) and He envelope ($0.15 - 0.3 M_{\odot}$) masses and find that, for those detonations on CO cores below $0.6 M_{\odot}$, explosions produce large quantities of ^{40}Ca , ^{44}Ti and ^{48}Cr , and very little ^{56}Ni . For a given CO core mass, the mass fraction in the ejecta of ^{56}Ni increases with the mass of the He shell. Additionally, ^{56}Ni mass fraction can be reduced by polluting the remnant’s envelope with CO - at $\sim 10^8 \text{ K}$, α capture onto carbon is faster than the $3-\alpha$ process, allowing carbon to effectively slow the nuclear reaction rate of He. Simulated light curves have a rise time of ~ 7 days, a ~ -11 to -18 peak bolometric magnitude, and highly differing late-time behaviour, depending on the mix of radioactive species produced.

Shen et al. (2010) and Woosley & Kasen (2010) also simulate He shell detonations in 1D, focusing on detonating thin ($\sim 0.02 - 0.1 M_{\odot}$) He shells on top massive cores ($0.6 M_{\odot}$ CO - $1.2 M_{\odot}$ ONeMg) to simulate .Ia SNe. Shen et al., however, also simulate detonations of $0.2 - 0.3 M_{\odot}$ envelopes over $0.6 M_{\odot}$ cores, and their resulting light curves and spectra are in general agreement with those of Waldman et al., despite having a different code and a more realistic detonation initialization (though they also do not consider core detonations). Resulting light curves are, again, highly varied. As an example, in their $0.6 M_{\odot}$ CO - $0.3 M_{\odot}$ He detonation,

$0.3 M_{\odot}$ is ejected (of which 65% is ^{56}Ni), with a average asymptotic velocity of $1.3 \times 10^4 \text{ km s}^{-1}$ and kinetic energy of $5.3 \times 10^{50} \text{ erg s}^{-1}$. The peak bolometric magnitude obtained is -18. Woosley & Kasen simulates the acutal He accretion process, and provide detailed analysis of the process leading from accretion to explosion. Their simulations reproduce light curves with a range of peak values and δm_{15} (number of magnitude drops 15 days after the start of the SN) similar to those found by Shen et al.. Ejecta velocities and spectroscopic features are also similar between the two papers. Woosley & Kasen (2010) also note that hotter CO WD accretors tend to produce weaker, faster explosions that resemble the He deflagrations mentioned in the previous section.

He shell detonation has been proposed as an explanation for fast, low-luminosity type Ib SNe that produce very little ^{56}Ni , have low ejecta masses and have moderate ejecta velocities, and spectroscopically show strong lines of He, Ca and Ti (Perets et al. 2010; Waldman et al. 2010). The prototype of this class is SN 2005E, which had (assuming only ^{56}Ni -decay powered light curves) $0.28 M_{\odot}$ of ejecta, $0.003 M_{\odot}$ produced, and $1.1 \times 10^4 \text{ km s}^{-1}$ average ejecta velocity (Perets et al. 2010). While these explosions could be caused by core-collapse of $\sim 10 M_{\odot}$ stars, these SNe appear from both young and old stellar populations, and debate is still ongoing regarding the environments that spawn such SNe (Ibs also typically have far greater ejecta masses and greater nucleosynthetic output) (Kawabata et al. 2010; Perets et al. 2010; Waldman et al. 2010; Perets et al. 2011). Another class of fast SN, SN 2002bj-like SNe (peak B-band light ~ -18.5 , $0.15 M_{\odot}$ ejected - most of it ^{56}Ni , on order 10^{50} ergs kinetic energy), has also been proposed to be caused by He shell detonations due to their correlation with older stellar populations and their low ejecta masses (Perets et al. 2010). For SN 2002bj, however, the evidence for He in the spectrum is less conclusive than for SN 2005E (Perets et al. 2010; Poznanski et al. 2010).

Waldman et al. compared their models to the light curve of SN 2002bj, and light curve and spectrum of SN 2005E. While they cannot exactly reproduce the light curve and spectrum of SN 2005E, their 0.45 CO - 0.2 He detonation model can reproduce SN 2005E's peak-light (-15th mag) and ejecta velocities. On the other hand, the models have faster late-time declines, and faster evolving spectra, than SN 2005E. Though most observed features are replicated by the light curve, their strengths are not. Both facts suggest that SN 2005E had a somewhat different total ejecta mass (the model gives $\sim 0.2 M_{\odot}$; an estimate from observations assuming a light curve powered only by ^{56}Ni gives $\sim 0.28 M_{\odot}$) and composition. SN 2002bj-type light curves are either too bright at peak light, or decay too quickly, to fit well to the curves of either Waldman et al. or Sim et al. (2010), suggesting either alternative explosion mechanisms or the need for a more detailed study of He shell detonation parameter space.

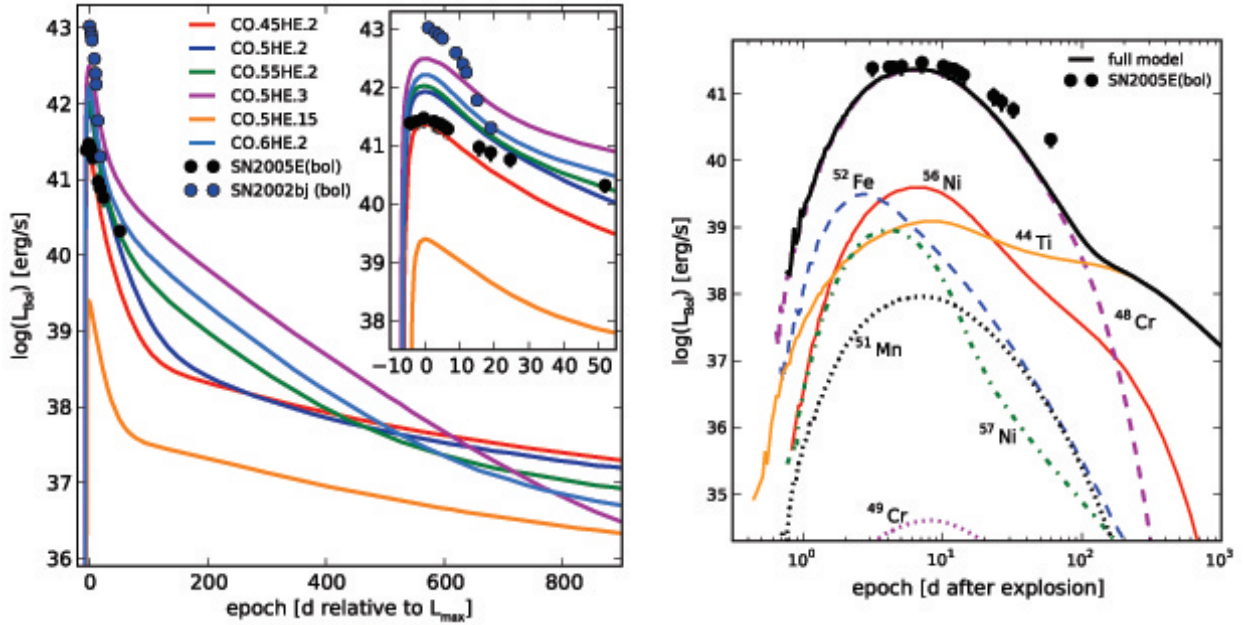


Fig. 9.— Left: bolometric light curves of 1D explosion models simulated by Waldman et al., compared to type Ib SN 2005E and SN 2002bj. Error bars of the observed SN include errors due to unobserved bands. Right: light curve for SN 2005E compared with a $0.45 M_{\odot}$ CO core, $0.2 M_{\odot}$ He envelope remnant (Waldman et al.’s best fit to SN 2005E), along with the light curve contributed by each radioactive decay chain. Note that at early times the light curve is dominated by ^{48}Cr , and at late times by ^{44}Ti .

Brown et al. (2011) study a sample of 12 extreme low mass (ELM; $\leq 0.25 M_{\odot}$) He WDs, 11 of which are in binary systems⁵. From this sample they determine the combined merger and stable mass transfer system creation rate to be $4 \times 10^{-5} \text{ yr}^{-1}$ (which they note is likely an underestimate), of which they estimate, by using Eqn. 6, that $\sim 30\%$ of this rate will be He-CO WD mergers, meaning the He-CO WD merger rate is $\sim 1 \times 10^{-5} \text{ yr}^{-1}$. Supplementary material from Perets et al. give the rate of calcium-rich SNe to be $\sim 7\%$ of the total SN Ia rate, which Brown et al. give as 5×10^{-3} , meaning that mergers between low mass He and CO WDs only accounts for a fraction of calcium-rich SNe. Other progenitors may include mergers involving heavier He WDs (much more common, cf. Secs. 1.1 and 3.2), He transfer from non-WD companions, or other detonation mechanisms⁶.

4.2.3. *He Detonation With CO Detonation*

If a detonation were to occur in He, it is possible for this detonation to propagate into the CO core as a edge-lit (i.e. CO-He interface-lit) CO detonation, disrupting the entire WD. An outward propagating He detonation could also, via inward propagating shockwaves, compress the CO core to the point at which its centre ignites. An He detonation triggering a CO detonation is known as the “double-detonation” scenario, and has been well-studied (cf. references in Woosley & Kasen (2010), Fink et al. (2007) and Fink et al. (2010)). Woosley & Kasen find very little difference in outcome between edge-lit and compressional double-detonations.

A significant issue discussed by Woosley & Kasen is that for a compressional detonation the inward shocks must converge in a region less than 100 km across to light the CO detonation. Current 1D simulations artificially satisfy this convergence, but if an He detonation is to be reached the He nuclear runaway layer must fragment into small sections that do not communicate with each other, and whether a simultaneous detonation at multiple points is possible is still an open question. A probable outcome is an asynchronous detonation of several extended regions in the runaway layer, and the resulting lack of shockwave convergence makes a CO detonation more difficult (Woosley & Kasen 2010). An issue for the edge-lit detonation is propagation of the He detonation wave into CO core, which is a function of density, altitude of the He detonation from the CO core, and the degree of He-CO mixing

⁵Brown et al. make the case that the 12th is likely a pole-on binary system, since low mass He WDs cannot be made through single-star evolution

⁶Including mergers of ELM He WDs with other HE WDs would approximately double Brown et al.’s rates.

at the interface between the two layers. Woosley & Kasen note that both problems require a more detailed understanding, and treatment in 3D simulations.

Fink et al. (2007) perform 2D simulations (z-axis vs. radius coordinates) of compressional detonations from various initial flame geometries, such as single point detonations, spherical shell detonations, and single/multiple torus detonations. Their initial system consists of either a $0.8 M_{\odot}$ CO core with a $0.2 M_{\odot}$ He shell, or a $0.9 M_{\odot}$ core with a $0.1 M_{\odot}$ shell. They also followed up a single point detonation using a full 3D cartesian simulation. They find that the majority of their detonations result in a secondary core explosion, and they argue that due maximum density being resolution limited, it is likely all their simulations should lead to explosions if their resolution was infinite⁷. Their explosions are comparable to (though somewhat weaker than) normal SNe Ia: all $1.0 M_{\odot}$ are ejected, with an average speed of $\sim 10^4 \text{ km s}^{-1}$, and $\sim 0.4 M_{\odot}$ ^{56}Ni is produced. Their 3D result is very similar to their 2D results, only producing $0.05 M_{\odot}$ more ^{56}Ni . Follow-up work (still in 2D) was presented in Fink et al. (2010) with a refined nuclear reaction chain. The results from Fink et al. (2007) still hold, except that more of the He shell burned into IMEs during the explosion rather than ^{56}Ni , which would help make the explosion look more like an SN Ia (see below). Again the entire star is ejected, about $0.2 - 1.1 M_{\odot}$ of ^{56}Ni is produced (highly dependent on progenitor mass) and 10^{51} ergs asymptotic energy is released. These results has been challenged by Woosley & Kasen, who state that Fink et al. uses a completely convective envelope, while their simulations of comparable initial masses, using more correct initial conditions where convection is frozen-out, burn He all the way to ^{56}Ni . Note that Fink et al. (2007) and Fink et al. (2010) use perfect mirror symmetry and assume complete burning from He to Ni during explosions, both somewhat unrealistic assumptions that significantly increase the chances of detonation (Guillochon et al. 2010).

Traditionally double-detonations have been contenders for SN Ia progenitors. Model spectra from such events, however, do not match spectra of observed SN Ia - IME lines are too weak in the models, owing to the nuclear processing of the outer He layer to ^{56}Ni (Woosley & Kasen 2010; Fink et al. 2007; Van Kerkwijk et al. 2010; Howell 2010). Still, one supernova, the over-luminous SN 1991T, did have large amounts of ^{56}Ni in its outer layers, and may have been a double-detonation (Fink et al. 2007). Centre-lit CO detonations without any He envelope have recently been shown by Sim et al. (2010) to look much like SNe Ia, which suggests that if a very thin envelope were to start a double detonation the resulting SN would more closely resemble an SN Ia (Howell 2010). Woosley & Kasen set an upper limit to the mass of the envelope at $\sim 0.05 M_{\odot}$. Both Woosley & Kasen and Fink et al. showed

⁷This is due to the fact that Fink et al. find that all of their initial flame geometries eventually produce inward propagating shocks that are roughly spherically symmetric.

that detonating shell masses lower than this value may still cause a double-detonation.

It is interesting to note that if double detonations produce explosions that do not look like SN Ia, we should see a significant fraction of SN with similar brightnesses to SN Ia, but with differing spectroscopic features. That we do not see this either means that double-detonations do not work as we understand them, all double-detonations are of the thin-envelope variety, or the conditions for reaching detonation are not often created during slow accretion of He onto CO WDs.

5. Carbon-Oxygen WD Mergers With Carbon-Oxygen Companions

5.1. ONeMg WD Formation

Rapid accretion of the remnant disk onto the core following a CO-CO merger may result in off-centre carbon ignition, which forms a carbon burning shell. The energy released during nuclear burning is either emitted as neutrinos, or retained by the WD and conducted inward from the shell (Saio & Nomoto 1998). Therefore the shell propagate inwards, turning the remnant into an ONeMg WD over a timescale of 10^3 - 10^4 yr (Yoon et al. 2007; Saio & Nomoto 1998). Saio & Nomoto simulate the evolution of the burning shell assuming an accretion rate of $1 \times 10^{-5} M_\odot \text{ yr}^{-1}$, and find no explosive phenomenon. Once an ONeMg WD is formed, an accretion-induced collapse (AIC) is generally thought to follow if the WD is too massive or if accretion continues (Yoon et al. 2007; Saio & Nomoto 1998). AICs are described in Sec. 6.

5.2. Type Ia Supernovae from CO-CO Mergers

The most spectacular transient that could potentially come of a CO WD merger is undoubtedly a type Ia supernova (SN Ia). The light curves of SNe Ia and the physical processes that can be discerned from them is a well-studied subject, and will not be covered here in detail. In general for SN Ia, the total ejecta mass is the mass of the progenitor WD or WD binary, ~ 0.4 - $0.7 M_\odot$ of ^{56}Ni is produced, and $\sim 10^{51}$ ergs of energy is released (Blinnikov et al. 2006). Excellent review articles on the subject that do go into much more detail include Howell (2010) and Hillebrandt & Neimeyer (2000).

The canonical progenitor of an SN Ia, however, is a CO WD accreting mass stably from a non-degenerate companion (rather than another CO WD) (Hillebrandt & Neimeyer 2000; Howell 2010). As the Chandrasekhar mass M_{Ch} is approached, temperatures and pressures

near the core of the CO WD exceed what is required to ignite carbon fusion, and a runaway nuclear process results (Hillebrandt & Neimeyer 2000; Howell 2010). This picture has several shortcomings. It firstly requires physical fine-tuning: a precise accretion rate during stable mass transfer is required to prevent recurring novae or stable AGB-like nuclear shell burning (neither of which lead to a massive explosion) (Van Kerkwijk et al. 2010; Howell 2010). Binaries that accrete at the correct rate should emit low-energy X-rays, and the number of such “super-soft” X-rays sources observed in the universe is far outweighed by the number needed to account for the observed SN Ia rate (Van Kerkwijk et al. 2010; Howell 2010). If an M_{Ch} WD were to experience nuclear runaway, an ad-hoc deflagration-to-detonation transition is needed in order to obtain ejecta velocities and compositions consistent with observed SNe Ia (Hillebrandt & Neimeyer 2000; Howell 2010). This suggests considering double-degenerate mergers as a channel for creating SNe Ia.

5.2.1. Chandrasekhar Mass CO Detonations

The Chandrasekhar double-degenerate merger picture is one where, following the merger, disk accretion drives the core to the Chandrasekhar mass, generating an explosion. One issue that has plagued this model is achieving M_{Ch} without igniting off-centre carbon burning, which leads to an ONeMg WD (Yoon et al. 2007; Loren-Aguilar et al. 2009). As noted earlier in Sec. 4.2, accretion is critically dependent on the timescale for viscous transfer of angular momentum between the disk and core, and as a result could range from as low as $10^{-11} - 10^{-14}$ to as high as $10^2 M_{\odot} \text{ yr}^{-1}$ (Loren-Aguilar et al. 2009). Yoon et al. perform a very detailed investigation of a 0.6-0.9 M_{Ch} CO-CO merger remnant evolution, and determined that if the rate of angular momentum loss (to the disk or via gravitational radiation) is slow enough that neutrino cooling can balance heating from loss of rotational support, and if $\dot{M}_{\text{acc}} \lesssim 5 \times 10^{-6} - 10^{-5} M_{\odot}/\text{yr}$, an M_{Ch} core may be created. It may also be possible, from variations in the angular momentum loss timescale, to ignite carbon fusion at masses slightly above or below M_{Ch} , giving variation to SN Ia explosion strengths. Note that the resulting star must still trigger a deflagration-to-detonation transition.

If the deflagration-to-detonation occurs off-centre, an asymmetric ejecta composition results. Sim et al. (2007) study how light curves are affected by this asymmetry using a toy explosion and radiative transfer model, and find that, in their most extreme asymmetric models, peak light can vary by as much as ~ 1.5 mag while time to peak light may vary by ~ 8 days. This variation is due to the fact that there is more material enshrouding the ^{56}Ni on one side of the star. Sim et al. (2007) note that such SNe Ia are likely to be rare, as if they were common the tight correlation between explosion bolometric flux vs. recession

velocity would have much more noise. This effect is then likely confined to a peak light variation of ~ 0.5 mag and rise time variation of ~ 3 days, making asymmetry a second-order effect. Asymmetry in SNe Ia is also a well-studied topic (cf. for example references in and to Sim et al. (2007)).

Fryer et al. (2010) model in 1D the detonation of an M_{Ch} WD surrounded by envelopes of various masses and compositions of either CO or He. Such a situation would be expected for a merger, and not for a single-degenerate or stable-mass transfer system (since the secondary would not surround the primary). They find (see Fig. 10) that enshrouding delays, compared to normal SN Ia, UV emission from the initial outburst, and shock heating (generally ignored in SN Ia simulation) further enhances and broadens the UV light curve, sometimes even creating a double-peaked curve. V-band emission is also significantly broadened compared to normal SN Ia. There are also early spectral differences between the models and observed SNe Ia. Fryer et al. conclude that such enshrouded systems should not produce ordinary SNe Ia, and suggest that merger rates of different massed WDs may conspire to make it so that the majority of merger CO WD binaries barely exceed M_{Ch} , minimizing the effects they see in their simulations. Also, notably, a few SNe Ia, such as SN 2002ic and SN 2005gj do appear to have been Ia inside extended envelopes (another section of this report suggests a different interpretation of these SNe).

A detonation carries its own signature distinct from the canonical SN Ia light curve. Piro et al. (2010) calculate that the shockwave from a detonation breaking out from the surface layers of the WD should create a 10^{-2} s burst of hard X-rays with peak luminosity $\sim 10^{44}$ erg s $^{-1}$, followed by a cooling tail. Peak absolute magnitude in the V band is around -9 to -10, and occurs one day after the detonation. Piro et al. add that the visibility of this transient will depend on the WD radius at the time of the detonation, and ^{56}Ni decay soon after the explosion. Höflich & Schaefer (2009) suggests the X-ray burst energy peak luminosity is closer to $10^{48} - 10^{50}$ erg s $^{-1}$, though these numbers may drop to the level of Piro et al. if expansion and adiabatic cooling over the diffusion time are taken into account. Fryer et al. study shock breakout in an enshrouded SN Ia and find that the X-ray emission (like the UV emission described above) is delayed and spread out over a longer period of time, and the peak luminosity decreases, as the mass of the envelope surrounding the Ia increases. They note, however, that the mass distribution is at least as important as the amount of mass, and therefore using shock breakout to determine whether the SN Ia is enshrouded requires further investigation.

If the two WD masses are nearly the same, a different SN Ia channel emerges. Pakmor et al. (2010) simulate the merger of two 0.89 CO WDs, and track points of high temperature and density near the core of the star. Finding a point with density 3.8×10^6 g cm $^{-3}$ and

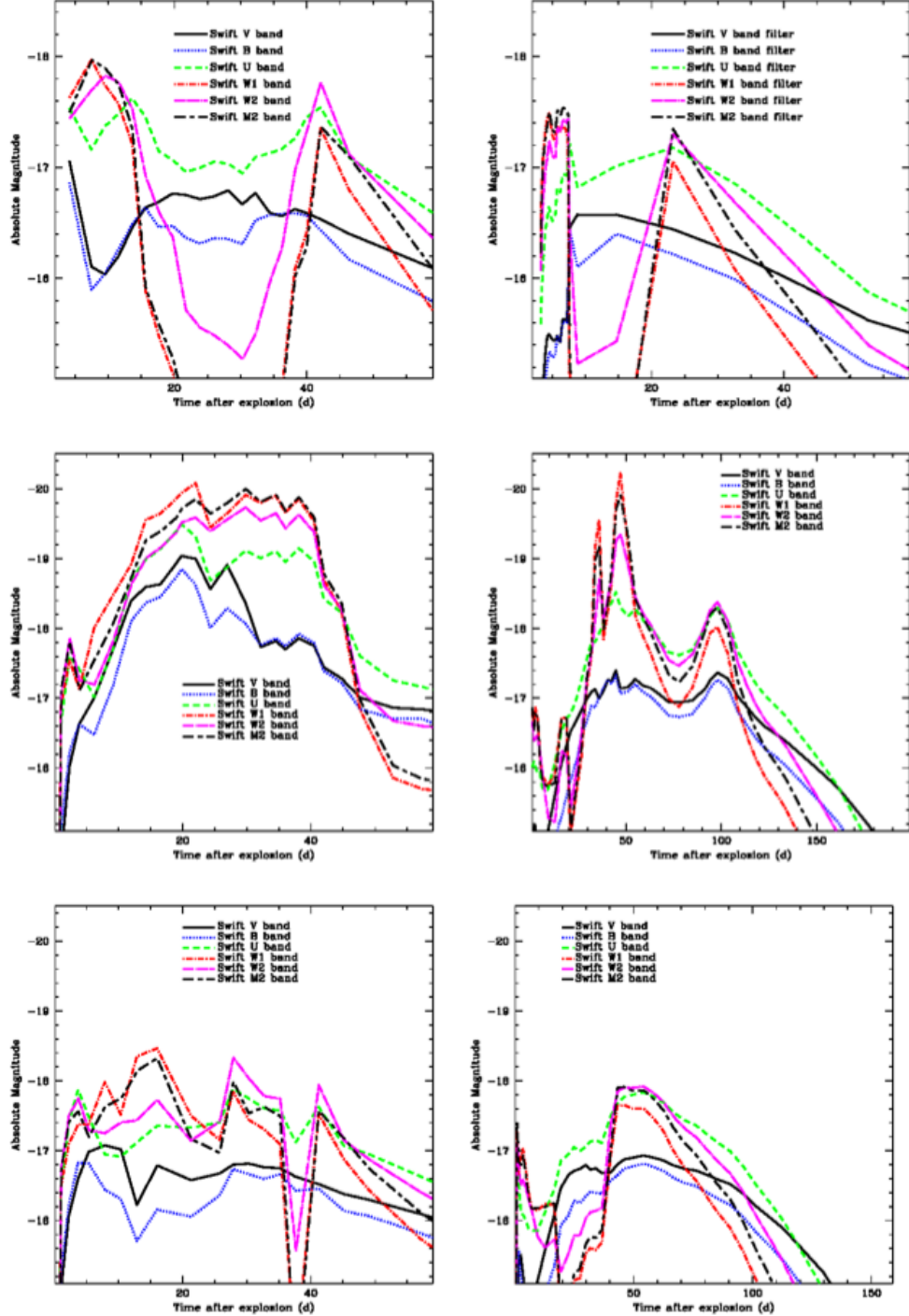


Fig. 10.— Simulated light curves of enshrouded SNe Ia with differing extended envelope masses and compositions, for a number of *Swift* visual and UV bands. All the plots on the left column are for He envelopes, and the right for CO envelopes; the envelope masses are 0.1 (top column), 0.35 and 0.7 M_{\odot} . Note that in a number of plots the U, W and M bands appear to have either a plateau of emission or a double peak. From Fryer et al. (2010), their Fig. 9.

temperature 2.9×10^9 K, they transfer the remnant model onto a grid-based hydrodynamic code and artificially detonate the point. The result is a sub-luminous, low-velocity explosion with a peak B-band magnitude of ~ -17 following a rise time of around 15 days, asymptotic kinetic energy of 1.3×10^{51} ergs, and $1.8 M_{\odot}$ of ejecta, with $0.1 M_{\odot}$ of that being ^{56}Ni . They also note incomplete silicon burning over a large fraction of the WD leads to well-mixed iron and silicon group elements, which is not seen in the layered ejecta of ordinary SNe Ia. Pakmor et al. compare their results to 1991bg-like underluminous SNe Ia, and find both light curves and spectra to be in very good agreement. They also use a population synthesis model to determine that such mergers should account for 2-11% of SNe Ia, which is in range of the fraction of observed SNe Ia that are 1991bg-like, regardless of whether normal SNe are created by the single or double-degenerate Chandrasekhar channels. Follow-up work (Pakmor et al. 2011) shows that the equal mass condition for a detonation could be relaxed to $q = \sim 0.8$, although unequal mass mergers should have higher ^{56}Ni yields (see Sec. 5.2.2) and hotspots produced are off-centre. Note this picture is significantly different than the Chandrasekhar model discussed above - the detonation occurs during the merger itself, and not during the accretion phase afterward. See Fig. 11 for details.

5.2.2. Sub-Chandrasekhar Mass CO Detonations

On the other hand, the majority of CO-CO WD mergers will result in sub-Chandrasekhar mass remnants with hotspots too cold to ignite runaway carbon fusion (Van Kerkwijk et al. 2010; Loren-Aguilar et al. 2009). As noted earlier, the remnant disk could accrete onto the core in a matter of hours. Van Kerkwijk et al. argue that if accretion were so quick, compressional heating would be high enough to create the conditions for carbon fusion at the centre of the remnant core, resulting in a detonation. This sub-Chandrasekhar picture has the advantage of not requiring a deflagration-to-detonation transition, and conveniently explains why SN Ia peak luminosity decreases with increasing progenitor age. Moreover, surveys and population synthesis show the rate of SN Ia from single and double degenerate Chandrasekhar channels combined is less than half the observed SN Ia rate, while the total rate of CO-CO WD mergers regardless of total mass is more than the SNe Ia rate (Van Kerkwijk et al. 2010; Sim et al. 2010). The lack of an He envelope negates the ejecta stratification problem that has historically plagued double-detonation models (Van Kerkwijk et al. 2010; Howell 2010; Sim et al. 2010). See Fig. 12.

One might expect that since Pakmor et al.’s 0.9-0.9 CO WD merger only produced $0.1 M_{\odot}$ of ^{56}Ni , the detonation of even lighter remnants would be very faint, but ^{56}Ni production is a strong function of remnant central density. An equal-mass 0.9-0.9 M_{\odot} merger remnant

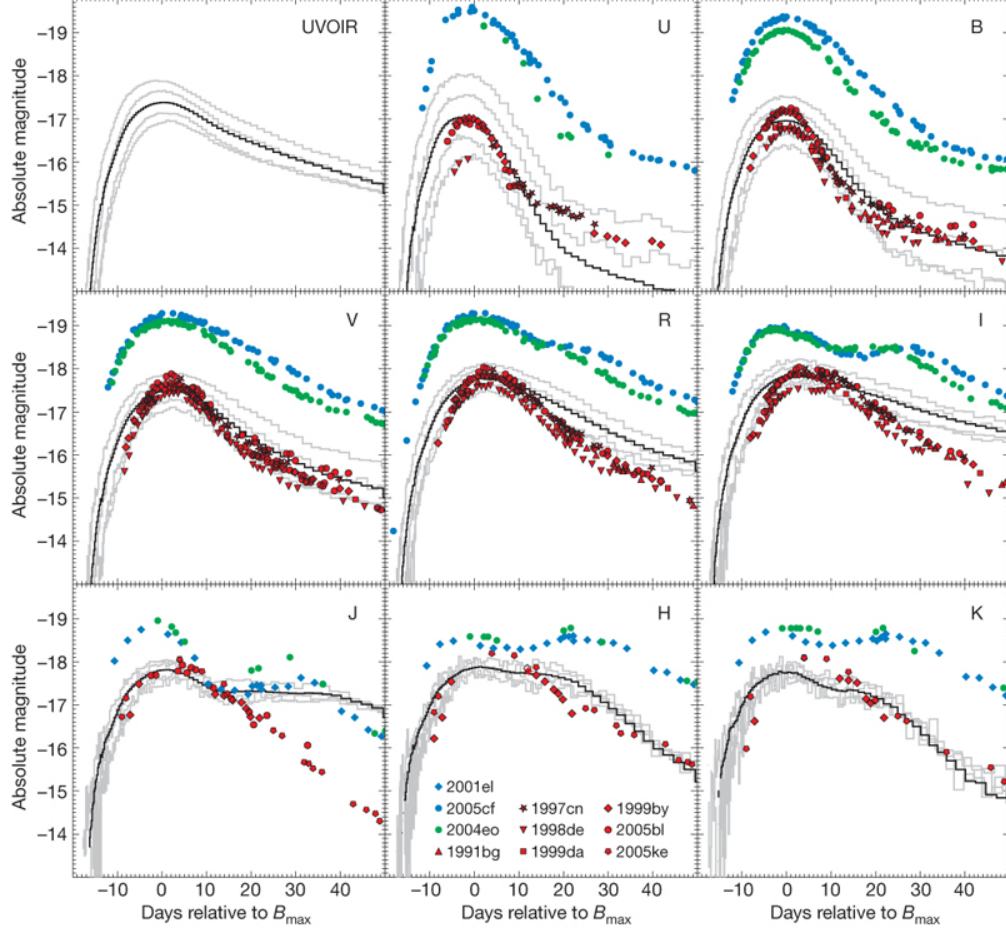


Fig. 11.— Comparison of synthetic light curves from a simulated double-degenerate merger SN Ia with a number of observed 1991bg-like SNe Ia curves. As the detonation is not spherically symmetric, the shape of the curve depends on viewing angle, and four solid grey curves have been plotted to indicate the distribution of light curves arising from this asymmetry. The solid black curve is the angle-averaged light curve. Blue points represent observed light curves for ordinary SNe Ia 2001el, 2005cf and 2004eo, while red points indicate light curves for 1991bg-like SNe Ia. $T = 0$ is set to the B-band maximum. Note that normal supernovae have a secondary maximum in the near-IR, which is not reproduced by either observed 1991bg-like SNe Ia or the synthetic curve. The synthetic curve does not drop as quickly as observed light curves in the optical and near-IR following peak light. From Pakmor et al. (2010), their Fig. 2.

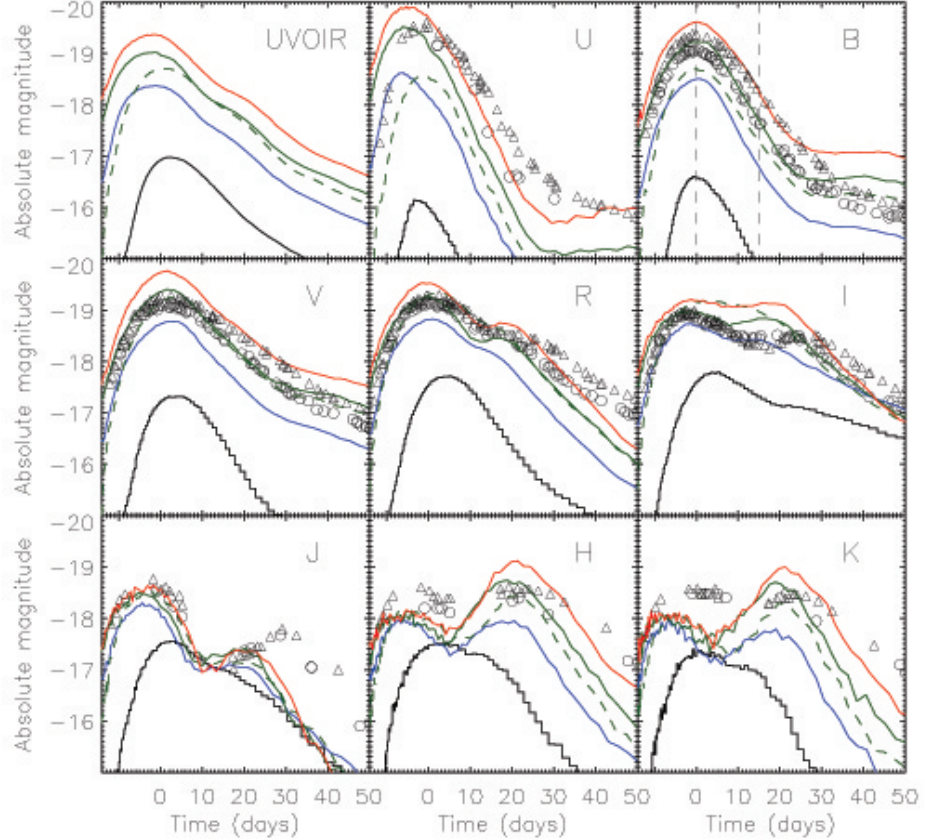


Fig. 12.— Comparison of synthetic light curves from simulated centre-lit detonations in $M = 1.15, 1.06, 1.06$ (polluted with Ne), 0.97 and $0.88 M_{\odot}$ CO WDs (red, solid green, dashed green, blue and black, respectively) and observed light curves of SN 2004eo and SN 2005cf (circles and triangles, respectively). Curves tend to drop too quickly after peak light, though Sim et al. (2010) note this may be due to how radiative transfer is treated. Traditionally the sub-Chandrasekhar picture involves the merger of a CO WD and an He WD, which is described in Sec. 4. These models, having no He envelope, differ from previous models that show ^{56}Ni stratification that does not agree with observation. From Sim et al. (2010), their Fig. 2.

is significantly less dense near its core than a 0.9-0.8 remnant, which means that mergers of unequal mass binaries will generally result in more luminous explosions than equal-mass binaries of the same total mass (Pakmor et al. 2011; Van Kerkwijk et al. 2010).

This picture relies critically on hot-spots being near the centre of the remnant core, and on accretion being on the timescale of hours, and therefore it is an open question how much fine-tuning is required for it to work.

5.3. Other Types of Explosions

As is obvious from above, the parameter space of all CO-CO mergers is significantly larger than the space of those mergers that create SNe Ia. Even if sub-Chandrasekhar mass mergers cannot lead to canonical SNe Ia, they should also still lead to transients of some sort (Pakmor et al. 2010).

5.3.1. Pure Deflagration of a Chandrasekhar Mass CO WD

If for some reason a deflagration-detonation transition does not occur, a pure deflagration could result. Blinnikov et al. (2006) model a pure deflagration starting at the centre of a M_{Ch} WD. The flame propagates outward, generating turbulence that increases the flame propagation velocity. This runaway process eventually consumes and disrupts the entire star. Blinnikov et al. show that a pure deflagration produces around 0.2 to 0.4 M_{\odot} of ^{56}Ni , as well as 0.35 to 0.65×10^{50} ergs of KE. Peak light in B-band is about -18 to -19 mag, and the rise time is ~ 17 days. ^{56}Ni is well mixed with IMEs, and there is an excess of unburned material travelling at low velocities. Variation in nickel and energy produced is due to differing central densities and chemical compositions of the WD progenitors. Blinnikov et al. find that while synthetic UVB light curves match well with weak SNe Ia that produce below 0.4 ^{56}Ni , the near-IR has too slow a rise time and does not drop quickly enough following peak light (leading to the bolometric light curve evolving too slowly compared with observations), while the U-band has too fast a rise time and drops too quickly. Additionally, the near-IR curves lack secondary maxima after peak light that are normally seen in observed SNe Ia (Blinnikov et al. 2006; Phillips et al. 2007). Blinnikov et al. state their models has known shortcomings, and that more refined deflagration models may result in more stratification of ejecta and faster moving ejecta, which should help resolve many of these issues.

Due to the low kinetic energies and amounts of ^{56}Ni in the ejecta of a pure deflagration, they are contenders for producing SN 2002cx-like supernovae. These underluminous

supernovae have low expansion velocities, no secondary maximum in the light curve, and significantly mixed ejecta, all consistent with pure deflagrations (Phillips et al. 2007). Phillips et al. (2007) compare one of Blinnikov et al. (2006)’s models to the light curve of SN 2002cx-like supernova SN 2005hk, and obtain reasonably good fitting, except for a small delay in peak light, and deviation from observation in the IR, and in other bands at late times. They believe refinements in radiative transfer codes and fine-tuning of the initial conditions can lead to better fits⁸. It should be noted that some SNe Ia, such as SN 2008ha, are too underluminous to be described by pure deflagrations. Foley et al. (2009) show that SN 2008ha had a peak luminosity of $\sim 10^{41}$ ergs, a kinetic energy of 2×10^{48} ergs, an ejecta velocity of 2000 km s^{-1} and an ejected mass of $0.15 M_{\odot}$ of matter, $4 \times 10^{-3} M_{\odot}$ of which was ^{56}Ni . This is far too little kinetic energy and mass to be a deflagration (Foley et al. 2009).

If the pure deflagration is highly asymmetric (i.e. the entire star explodes but is burned to ^{56}Ni largely on only one side), then asymmetry effects appear. Sim et al. (2007) simulate a pure deflagration creating $0.448 M_{\odot}^{56}\text{Ni}$ with such an asymmetry, and find peak magnitude variations of ~ 0.5 mag.

5.3.2. Failed Deflagrations

Failed deflagrations of Chandrasekhar mass WDs can also occur. Calder et al. (2004) and Livne et al. (2005) both find that for a single off-centre ignition point, the resulting hot ash bubble formed rises very quickly to the surface of the WD, leaving most of the star unburned. Surface velocities for the hot bubble range from ~ 5000 to $\sim 10000 \text{ km s}^{-1}$. From Calder et al. (2004), about 2% of the star is burned to iron peak elements (about twice as much is burned to IMEs), and only 0.2% of the star actually reaches escape velocity. This highly asymmetric explosion, if it managed to eject more material, would be consistent with the properties of SN 2008ha (Foley et al. 2009). (SN 2008ha is also potentially consistent with a transient caused by an AIC; see Sec. 6.)

⁸Deflagrations should have strong OI and CI forbidden lines due to an excess of low-velocity unburned material; this is not seen in SN 2002cx-like SN, though higher resolution deflagration simulations appear to reduce the discrepancy (Phillips et al. 2007).

6. Oxygen-Neon-Magnesium White Dwarf Mergers

Due to their mass, it is likely that the merger of an ONeMg WD with any companion will create a super-Chandrasekhar mass remnant. The consensus for such mergers is they are more likely to lead to accretion-induced collapse (AIC) than an explosion, though the matter is still not completely resolved (Yoon et al. 2007; Fryer et al. 2010; Dessart et al. 2006). Taubenberger et al. (2011) note an ONeMg triggered to detonate by an “external event” may explode instead of collapsing, and mention it as a possible explantion for the very bright ($\sim 10^{43}$ erg s $^{-1}$), slow-decaying SN 2009dc, which apparently ejected over 1.8 M $_{\odot}$ of ^{56}Ni at relatively low kinetic energies. It is also worthwhile to note that according to Fig. 1 it is plausible to have an He-ONeMg WD binary whose total mass is below the Chandrasekhar mass, but such a system would interact via stable mass accretion, according to Sec. 1.2. From the simulations of Loren-Aguilar et al., a 0.6 M $_{\odot}$ CO - 1.2 M $_{\odot}$ ONeMg WD merger will result in carbon nuclear processing, but any runaway nuclear reactions appear to be quenched. We did not find any simulations of runaway CO burning on an ONeMg WD.

The optical transient of the AIC itself was simulated by Dessart et al. (2006). Their work showed that core collapse results in a shockwave that breaks out along the poles of the (rapidly spinning) WD, followed by a neutrino-driven wind concentrated along the poles that ultimately ejects $3 - 4 \times 10^{-3}$ M $_{\odot}$, depending on the mass of the initial WD, at speeds in the range of $1 - 3 \times 10^4$ km s $^{-1}$. About a quarter of the ejected matter is ^{56}Ni . The total energy of the explosion is on order $5 \times 10^{49} - 10^{50}$ erg. The time before gamma rays can escape the ejecta is short, and in all this is not a strong optical transient compared to SNe (Metzger et al. 2009). Note that earlier work by Fryer et al. (1999) predicted an order of magnitude higher total mass, energy and ^{56}Ni .

Metzger et al. (2009) propose a transient from a different source: following the AIC, the proto-neutron star will be surrounded by a $\sim 0.1 - 0.5$ M $_{\odot}$ Keplerian disk with an outer radius of $\sim 30 - 100$ km and a temperature in the MeV range. The disk will, due to MHD turbulence, hyper-accrete onto the NS at rates of up to ~ 1 M $_{\odot}$ s $^{-1}$; by conservation of momentum, part of the disk will be ejected. This disk will be proton-rich when it cools to below 1 MeV, and is efficiently synthesized into ^{56}Ni . Metzger et al. calculate 3×10^{-2} M $_{\odot}$ of ejecta, about a third of which is ^{56}Ni , forming by this process from a ~ 0.1 M $_{\odot}$ accretion disk. This outflow has similar energies and speeds ($\sim 10^{50}$ erg, $\sim 30,000$ km s $^{-1}$) to the AIC ejecta (Metzger et al. 2009). The light curve from this transient, which they call a “naked AIC transient” is shown in Fig. 13.

Metzger et al. note that for a double-degenerate merger leading to an AIC, significant amounts (~ 0.1 M $_{\odot}$) of WD material will remain in a thick torus at a radius of 10^4 km. When the AIC ejecta and accretion disk outflow strike this outer envelope, ejecta speeds will slow

from 3×10^4 km s $^{-1}$ to $3 - 10 \times 10^3$ km s $^{-1}$ while shock-heating the outer envelope up to 10 9 K, which synthesizes intermediate mass elements. The larger total ejecta mass and slower ejecta velocities increase the rise time of the transient from 1 day (the naked case) to \sim 10 days, as seen in Fig. 13 (Metzger et al. 2009). In addition to iron-peak elements, the AIC outflow should contain Cr, Kr, Se and Br (not commonly found in SNe), and interactions with the torus should add more intermediate elements which may, in total, constitute a spectrum unique to AICs (Metzger et al. 2009). The exact composition of the ejecta will depend on the composition of the WD that merged with the ONeMg WD, and therefore composition could distinguish the difference between an He, CO and ONeMg-ONeMg merger.

Fryer et al. (2009) simulated an enshrouded AIC at the centre of a merger remnant using a radiation-hydrodynamics code and values similar to Dessart et al. (2×10^{50} erg total energy, $0.02 M_{\odot}$ ejecta, $4 \times 10^{-3} M_{\odot}$ ^{56}Ni), and obtain a similar light curve to Metzger et al.’s schematic light curve (Fig. 13). A peak V-band magnitude of -16 was achieved in \sim 10 days. Fryer et al. (2009) also simulate an explosion with ten times the energy, mass and ^{56}Ni in accordance with Fryer et al. (1999), and obtain a peak V-band magnitude of -18.5, achieved also in \sim 10 days. In neither explosion do they recover line features that would be unique to AICs in the resulting spectrum. They also note that the high energies and low ejecta masses mean most of the ejecta is ionized and line emission is washed out - this occurs early on for their more powerful explosion, and after peak light for their weaker explosion.

MARTEN: It’s not clear from literature why the spectral features of Cr, Kr, Se and Br speculated by Metzger et al. are not recovered in Fryer et al. (2009)’s spectra. It’s not really stated by Fryer et al. (2009), though they most certainly know Metzger et al.’s work. You might also want to use Fryer et al.’s spectrum instead of the schematic from Metzger et al..

Such an “enshrouded AIC” transient could be responsible for SN 2008ha, whose rise time, peak luminosity, ejecta velocity, ejected mass and ejected ^{56}Ni are all within range of the corresponding values stated above. With $0.16 M_{\odot}$ ejected at speeds of $\sim 10^4$ km s $^{-1}$ and $\sim 0.02 M_{\odot}$ ^{56}Ni produced, and possible detection of Al II lines in its spectrum, SN 2010X is also an enshrouded AIC candidate (Kasliwal et al. 2010). It is not likely for this merger channel to explain all possible sub-luminous SNe Ia, as most others eject much more ^{56}Ni than can be formed from an AIC-related transient (Foley et al. 2009).

If the WD merger remnant rotates differentially, then any initial poloidal magnetic field will be greatly amplified through the magnetorotational instability. Dessart et al. (2007) show that the entire star consequently spins down by as much as 30%, and the rotational energy lost is fed into a magnetically driven wind substantially more powerful than the neutrino wind described above. Explosion energies then reach up to $\sim 10^{51}$ erg and ~ 0.1

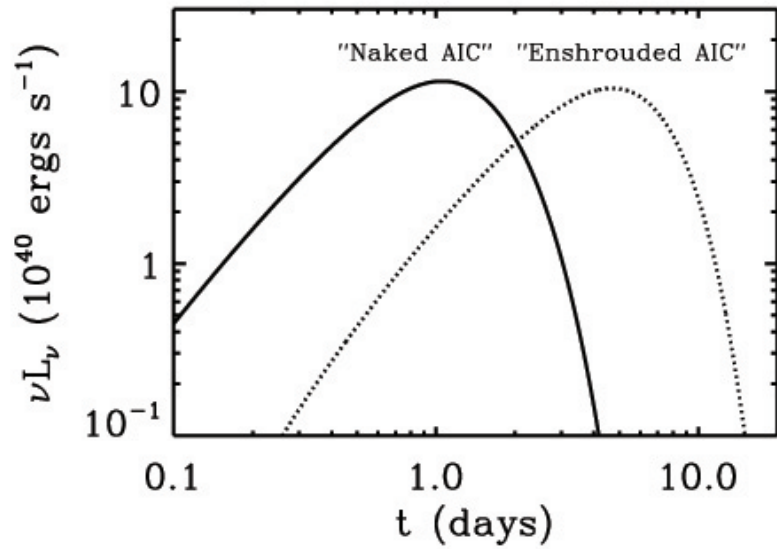


Fig. 13.— Model V-band light curve of two AIC transients. The naked transient (total mass $2 \times 10^{-2} M_{\odot}$, $10^{-2} M_{\odot}^{56}\text{Ni}$, $v = 3 \times 10^4 \text{ km s}^{-1}$), resulting from a stable mass transfer AIC, does not have an envelope left over from a WD merger, and rises and falls within a day's time. The enshrouded AIC transient (total mass $2 \times 10^{-1} M_{\odot}$, $10^{-2} M_{\odot}^{56}\text{Ni}$, $v = 10^4 \text{ km s}^{-1}$) results from a WD merger, and therefore has an envelope that stretches out the light curve over a week while keeping peak luminosity constant. These curves are consistent with Fryer et al. (2009)'s Fig. 7. From Metzger et al. (2009), their Fig. 2.

M_{\odot} is ejected, though negligible amounts of ^{56}Ni are created. The transient, therefore, is still fairly weak optically, and could instead be detected via neutrino and gravitational wave emission (Dessart et al. 2007).

Metzger et al. also speculate as to whether an AIC could emit a collimated relativistic outflow, thereby creating a short gamma-ray burst. One advantage to AIC-GRBs is that the late-time (around 10 - 100 s) x-ray tail seen in some short GRBs could plausibly be explained by late-time accretion of merger remnant material not carried away by the initial AIC outflow, or by magnetar outflows (assuming one is created by an AIC). See Dessart et al. (2007), however, for discussion as to why AICs likely will not create short GRBs unless the collapsing WD eventually forms a black hole. This 10 - 100 s x-ray emission might be seen regardless, and could be a target for x-ray survey missions (Metzger et al. 2009).

REFERENCES

- Bear et al. (2011). 2011arXiv1104.4106B
- Bildsten et al. (2007). 2007ApJ...662L..95B
- Blinnikov et al. (2006). 2006A%26A...453..229B
- Brown et al. (2011). 2011MNRAS.411L..31B
- Calder et al. (2004). 2004astro.ph..5162C
- Camenzind M., *Compact Objects in Astrophysics*. Heidelberg: Springer, 2007. 2007coaw.book.....C
- Clayton et al. (2007). 2007ApJ...662.1220C
- Dan et al.(2011). 2011arXiv1101.5132D
- Marius Dan, personal communication 4/28/2011
- D'Angelo et al. (2006). 2006AJ....132..650D
- Dessart et al. (2007). 2007ApJ...669..585D
- Dessart et al. (2006). 2006ApJ...644.1063D
- Eggleton (1983). 1983ApJ...268..368E
- Fink et al. (2010). 2010A&A...514A..53F
- Fink et al. (2007). 2007A%26A...476.1133F
- Foley et al. (2009). 2009AJ....138..376F
- Fryer et al. (1999). 1999ApJ...516..892F
- Fryer et al. (2009). 2009ApJ...707..193F
- Fryer et al. (2010). 2010ApJ...725..296F
- Gokhale et al. (2007). 2007ApJ...655.1010G
- Guerrero et al. (2004). 2004A&A...413..257G
- Guillochon et al. (2010). 2010ApJ...709L..64G

- Heber (2009). 2009ARA&A..47..211H
- Han (1998). 1998MNRAS.296.1019H
- Han & Webbink (1999). 1999A&A...349L..17H
- Han et al. (2002). 2002MNRAS.336..449H
- Han et al. (2003). 2003MNRAS.341..669H
- Höflich & Schaefer (2009). 2009ApJ...705..483H
- Howell (2010). 2010arXiv1011.0441H.
- Hillebrandt & Neimeyer (2000). 2000ARA%26A..38..191H
- Iben et al. (1998). 1998ApJ...503..344I
- Jeffery et al. (2011). 2011arXiv1103.1556J
- Justham et al. (2011). 2011MNRAS.410..984J
- Kawabata et al. (2010). 2010Natur.465..326K
- Kasliwal et al. (2010). 2010ApJ...723L..98K
- Livne et al. (2005). 2005ApJ...632..443L
- Loren-Aguilar et al. (2009). 2009A&A500.1193L
- Marsh et al. (2004). 2004MNRAS.350..113M
- Marsh (2011). 2011arXiv1101.4970M
- Metzger et al. (2009). 2009arXiv0908.1127M
- Moroni & Straniero (2009). 2009A%26A...507.1575P
- Motl et al. (2007). 2007ApJ...670.1314M
- Mannucci et al. (2005). 2005A%26A...433..807M
- Nelemans et al. (2001). 2001A%26A...368..939N
- Nelemans et al. (2001). 2001A%26A...365..491N
- Nelemans (2010). 2010Ap%26SS.329...25N

- Pakmor et al. (2010). 2010Natur.463...61P
Pakmor et al. (2011). 2011A&A...528A.117P
Pandey & Lambert (2011). 2011ApJ...727..122P
Perets et al. (2010). 2010Natur.465..322P
Perets et al. (2010). 2010arXiv1008.2754P
Perets et al. (2011). 2011ApJ...728L..36P
Phillips et al. (2007). 2007PASP..119..360P
Piro et al. (2010). 2010ApJ...708..598P
Poznanski et al. (2010). 2010Sci...327...58P
Rosswog (2007). 2007MNRAS.376L..48R
Saio & Jeffery (2000). 2000MNRAS.313..671S
Saio & Jeffery (2002). 2002MNRAS.333..121S
Saio & Nomoto (1998). 1998ApJ...500..388S
Segretain et al. (1997). 1997ApJ...481..355S
Shen et al. (2010). 2010ApJ...715..767S
Sim et al. (2007). 2007MNRAS.378....2S
Sim et al. (2010). 2010ApJ...714L..52S
Stamatellos & Whitworth(2008). 2008arXiv0810.1687S
Taubenberger et al. (2011). 2011MNRAS.tmp...61T
Tremblay & Bergeron (2009). 2009ApJ...696.1755T
Van Kerkwijk et al. (2010). 2010ApJ...722L.157V
Verbunt & Rappaport (1988). 1988ApJ...332..193V
Waldman et al.(2010). 2010arXiv1009.3829W
Woosley & Kasen (2010). 2010arXiv1010.5292W

Yoon et al. (2007). 2007MNRAS.380..933Y